SAND2020-3439

SANDIA REPORT
SAND2020-Draft
Printed July 2020

Sandia National Laboratories

Updated Available Drawdowns for Big Hill SPR Caverns - Model Including the Caprock Fault

Byoung Yoon Park

Prepared by
Sandia National Laboratories
Albuquerque, New Mexico
87185 and Livermore,
California 94550

Issued by Sandia National Laboratories, operated for the United States Department of Energy by National Technology & Engineering Solutions of Sandia, LLC.

Available to DOE and DOE contractors from
U.S. Department of Energy
Office of Scientific and Technical Information
P.O. Box 62
Oak Ridge, TN 37831

Telephone: (865) 576-8401
Facsimile: (865) 576-5728
E-Mail: reports@osti.gov
Online ordering: http://www.osti.gov/scitech

Available to the public from
U.S. Department of Commerce
National Technical Information Service
5301 Shawnee Rd
Alexandria, VA 22312

Telephone: (800) 553-6847
Facsimile: (703) 605-6900
E-Mail: orders@ntis.gov
Online order: https://classic.ntis.gov/help/order-methods/

ABSTRACT

This report updates the estimated values of the baseline available drawdowns for the caverns at the Big Hill storage facility, and an updated table listing the available drawdowns. An updated finite element numerical analysis model, which included a fault in the caprock layers, was constructed and the daily data of actual wellhead pressures and oil-brine interfaces was used. The number of available drawdowns for each of the Big Hill SPR caverns is estimated using the new model. All caverns are predicted to have five available drawdowns remaining from a geomechanical perspective. BH-101 and 105 have a region of concern at the floor edge and/or sloping floor, where tensile and dilatant stresses are predicted to occur during each workover. The tensile state is predicted to occur because of the geometries of the edge and floor. Therefore, geomechanical examination for two caverns would be recommended after a drawdown leach. The well integrity of each cavern is not investigated in this report. The estimates for the number of baseline available drawdowns are subject to change in the future as the knowledge of physical phenomena at the sites, and the further development of the models of geomechanical behavior at the sites, evolve over time.

Keywords: Available Drawdowns; Geomechanical Simulation; Salt Behavior

ACKNOWLEDGMENTS

This research is funded by SPR programs administered by the Office of Fossil Energy of the U.S. Department of Energy.
The author would like to thank Steven R. Sobolik, David B. Hart, and Courtney G. Herrick of Sandia provided technical reviews and valuable comments, and Sandia department manager Donald Conley and Sandia SPR project manager Anna C. Snider Lord who supported this work. As always, the support of Diane Willard of DOE is greatly appreciated. Paul Malphurs of DOE also is greatly appreciated, as is his comprehensive review of this report. This report has been improved by these individuals.

CONTENTS

LIST OF FIGURES

LIST OF TABLES

EXECUTIVE SUMMARY

This report updates the estimated values of available drawdowns for the caverns at the Big Hill storage facility, and an updated table listing the available drawdowns. This report follows up the comprehensive SAND report [Sobolik et al. 2018] that gave greater detail to the decisions behind the estimates for the Strategic Petroleum Reserve (SPR) caverns.

The estimates for the baseline available drawdowns for each of the Big Hill caverns have been updated based on the recently upgraded Big Hill geomechanical model [Park, 2019b]. The new estimates for Big Hill are summarized in the following table:

Cavern	Basis in 2014				Updated Geomechanics in 2020	Remarks
	2D P/D < 1	3D P/D < 1	Geomechanics	Best Estimate		
BH-101	3	3	5	3	5	Re-examine after a drawdown
BH-102	4	4	5	4	5	
BH-103	2	4	5	4	5	
BH-104	3	3	5	3	5	
BH-105	4	4	5	4	5	Re-examine after a drawdown
BH-106	4	4	5	4	5	
BH-107	3	4	5	4	5	
BH-108	2	5	5	5	5	
BH-109	4	5	5	5	5	
BH-110	4	5	5	5	5	
BH-111	3	4	5	4	5	
BH-112	3	3	5	3	5	
BH-113	3	3	5	3	5	
BH-114	3	5	5	5	5	

BH-101 and 105 have a regions of concern at the floor edge and/or on the sloping floor, where tensile and dilatant stresses are predicted to occur during each workover. The tensile state is predicted to occur because of the geometries of the edge and floor. Therefore, geomechanical re-examination for two caverns is recommended after a drawdown leach.

ACRONYMS AND DEFINITIONS

Abbreviation	Definition
3D	Three-Dimensional
2D	Two-Dimensional
BH	Big Hill
DF	Dilatant damage factor
DOE	U.S. Department of Energy
ECP	Engineering Change Process
E-W	East-West
FE	Finite Element
FFPO	Fluor Federal Petroleum Operations
ID	Identification
MMB	Million Barrels
Mbbl	Thousands of barrels
N-S	North-South
OBI	Oil-Brine Interface
P/D	Pillar to Diameter ratio
Sandia	Sandia National Laboratories
SPR	Strategic Petroleum Reserve

1. INTRODUCTION

This report updates the estimated number of available drawdowns for the caverns at the Big Hill (BH) storage facility. This report follows up on the comprehensive SAND report [Sobolik et al. 2018] that gave greater detail to the decisions behind the estimates of available drawdowns for the Strategic Petroleum Reserve (SPR) caverns.

A consensus has now been built regarding the assessment of drawdown capabilities and risks for the SPR caverns. This work began in 2014, when the SPR issued an Engineering Change Process (ECP), PM-00449, Baseline Remaining Drawdowns for all SPR Caverns. It described creating a technical baseline for all available drawdowns for each cavern considering pillar to diameter (P/D) ratios and other factors. These meetings led to the establishment of baseline values for available drawdowns for each cavern [Sobolik et al., 2014; Sobolik 2016]. Then in September 2017, Sandia National Laboratories (Sandia) was directed to update these reports annually to include a process to track the evolution of drawdown capacity for each cavern as operations are performed on them. This request was in response to legislation in 2015 directing the sale of SPR oil through the year 2025, to reduce the stored oil inventory at SPR from approximately 700 million barrels (MMB) to approximately 500 MMB. As a result, meetings were held between Sandia National Laboratories (Sandia), U.S. Department of Energy (DOE)/SPR, and Fluor Federal Petroleum Operations (FFPO; the SPR M&O contractor), to define the process that will be used to track volume changes and their impact on drawdown capacity [Sobolik et al. 2018].

The two-dimensional (2D) and three-dimensional (3D) P/D ratios for each of the BH caverns are described in detail in Rudeen and Lord [2013]. Computational results from Park and Ehgartner [2011] were used to determine the geomechanical drawdown limits. No BH caverns are currently predicted to exhibit a 2D P/D < 1.0 on the first raw water drawdown. The 14 SPR caverns at this site are predicted to be structurally stable well beyond the 5th drawdown leach [Park and Ehgartner, 2011]. However, the caverns in the numerical model for BH were simplified to cylindrical shapes. As a result, the 3D P/D-developed limits have been used to provide the best estimate assessment of the drawdown capacity for these caverns.

A new finite element (FE) numerical analysis model was constructed that consists of a realistic mesh capturing the sonar-measured geometries of Big Hill SPR site and the daily data of actual wellhead pressures and oil-brine interfaces was used [Park, 2019b]. The model contains the interbed between the caprock and salt top; and the interface between the dome and surrounding in situ rock to examine the interbed behavior in the most realistic manner. The fault, which was ignored for the simplification in previous report [Park, 2019a], is included in this model to perhaps better represent the large scale deformation considered in this study. The number of available drawdowns for each of the BH SPR caverns is estimated using the new model.

The well integrity of each cavern is not investigated in this report. Only the structural integrity of the caverns is examined at this time. The estimate of the number of baseline available drawdowns for the BH caverns in this report will be incorporated in future assessments of the available drawdowns for all the SPR caverns at four sites. Additionally, due to modeling constraints and the assumptions used to create these geomechanical models, an upper limit of five possible available drawdowns has been designated for all the SPR caverns. Many caverns that are shown through geomechanical analyses to have five baseline available drawdowns may actually have capacity for more than five, but will be limited to five for the present. The estimates for the number of baseline available

drawdowns are subject to change in the future as the knowledge of physical phenomena at the sites, and the further development of the models of geomechanical behavior at the sites, evolve over time.

2. SITE DESCRIPTIONS

Figure 1**Error! Reference source not found.** shows a plan view of the BH site with contour lines defining the approximate location of the salt dome top and the locations of fourteen SPR caverns currently in-use (101-114). The figure also specifies the undeveloped area north of the DOE property line (Sabine Pass Terminal). The horizontal shape of the dome is approximated as being elliptical. The major and minor ellipse axes are measured as approximately 7000 ft and 5800 ft, respectively.

The West-East cross-section #1 through the northern-most row of caverns (Cavern 101-105) provides a geologic representation near the middle of the dome (Figure 2). The site has a thin overburden layer consisting of sandy soil; and an exceptionally thick caprock sequence comprised of two layers. The upper caprock is comprised mainly of gypsum and limestone, whereas the lower caprock is mostly anhydrite. For numerical analysis purposes, the top layer of overburden is modeled as having a thickness of 300 ft, the upper caprock 900 ft thick, and the lower caprock 420 ft thick. The interbed layer of 20 ft thick is assumed to exist between the lower caprock and salt dome. The bottom boundary of the present analysis model is set at 6000 ft below the ground surface, so the height of salt dome is 4360 ft as shown in Figure 2.

A major fault (shear zone) extends approximately North-South along the entire length of the caprock and for an unknown depth into the salt. This fault zone has a pronounced effect on the subsidence measured above the site and is a consideration for future cavern placement [Ehgartner and Bauer, 2004]. The salt dome is essentially two large salt spines. The two masses of salt are operating somewhat independently, pushing up creating the shear zone separating the two spines and resulting in faulting in the caprock above. The shear zone is a region separating two salt spines, typically characterized by containing impurities, compositional changes, physical property variations, and possibly inclusions of hydrocarbons [Snider Lord, 2019].

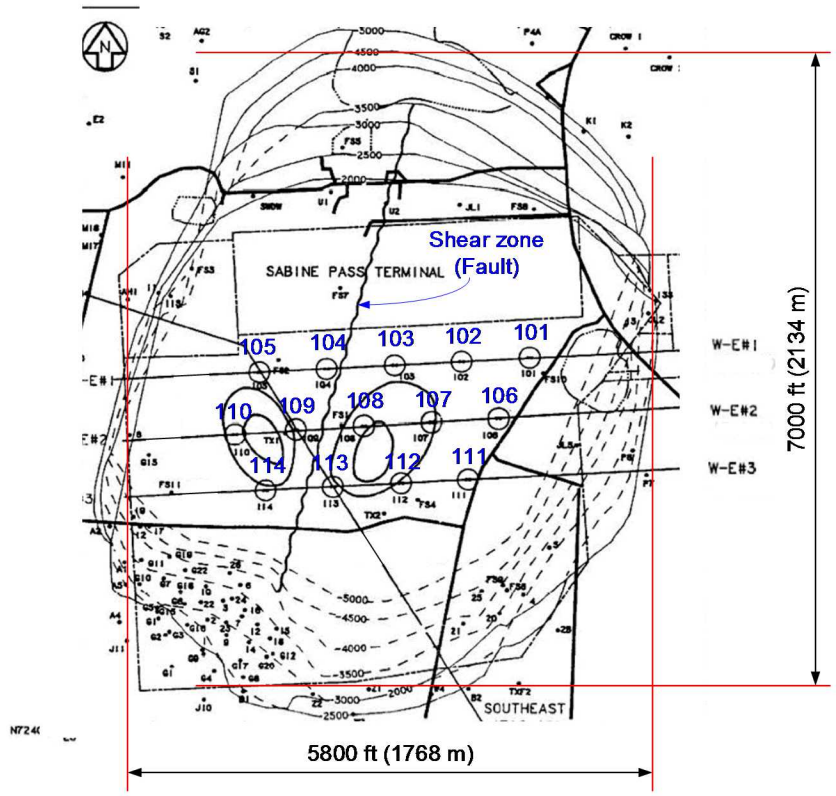

Figure 1. Big Hill site plan view [Magorian and Neal, 1988]

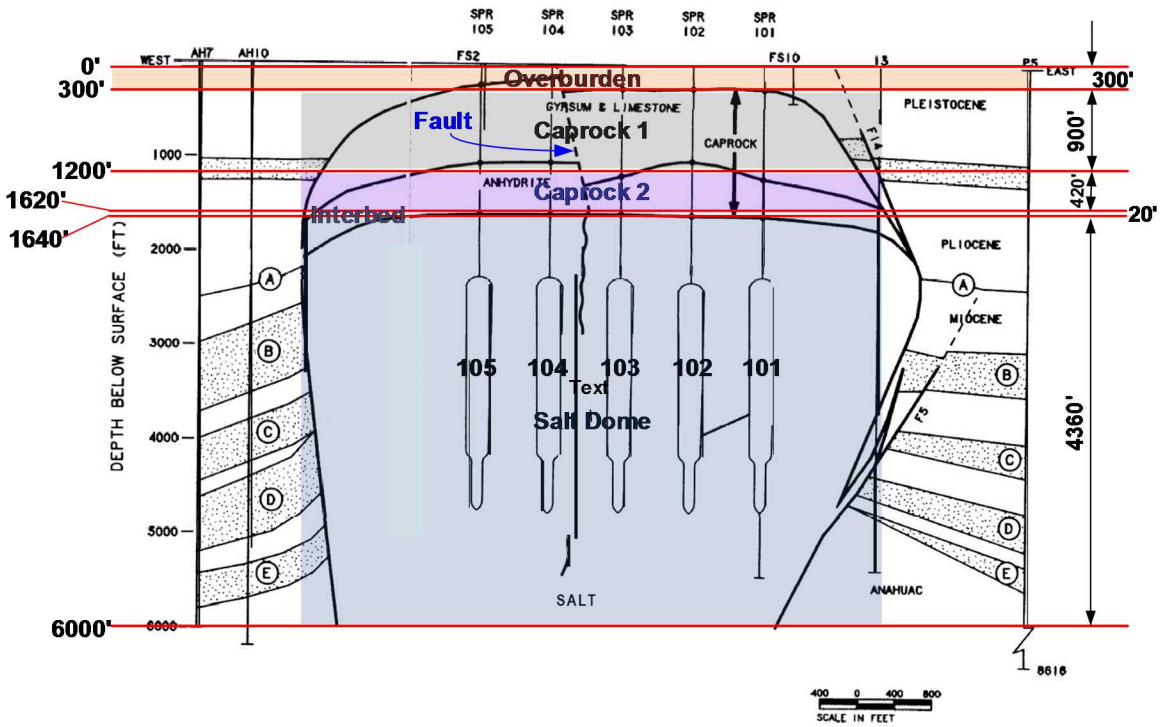

Figure 2. Cross-section (W-E #1 in Figure 1 Error! Reference source not found.**) near middle of dome [Magorian and Neal, 1988] looking North.**

3. MODEL DESCRIPTION

3.1. Finite Element Model

A 3D FE model capturing realistic geometries of BH site has been constructed using sonar and seismic survey data obtained from field investigations [Park, 2017a]. The model contains the interbed between the caprock and salt top; and the interface between the dome and surrounding in situ rock to examine the interbed behavior in the most realistic manner. The fault, which was ignored for simplification in a previous report [Park, 2019], is included in this model to better represent the large scale deformation considered in this study.

Figure 3 shows an overview of the finite element mesh of the stratigraphy and cavern field at BH. These cavern colors will correspond to the input histories and analysis result curves in the following sections. The element blocks in Figure 3 are combined into single FE mesh as shown Figure 4, which includes the boundary conditions for numerical analysis. The surrounding rock block encircles the caprock and salt dome blocks. The lengths of the confining boundaries are 14,600 ft in the N-S direction and 12,400 ft in the E-W direction. The boundary dimensions are determined by more than two times of the dome's range in each direction. The salt dome is modeled as being subject to a uniform regional far-field stress state acting from an infinite distance away. The sizes of the caverns are horizontally much smaller than the dome. Therefore, the North and South sides of far-field boundary are fixed in Y-direction, and the East and West sides are fixed in X-direction. The bottom is fixed vertically. The top surface and four sides are vertically free. The acceleration of gravity used in the model is 9.81 m/s^2 (32.174 ft/s^2).

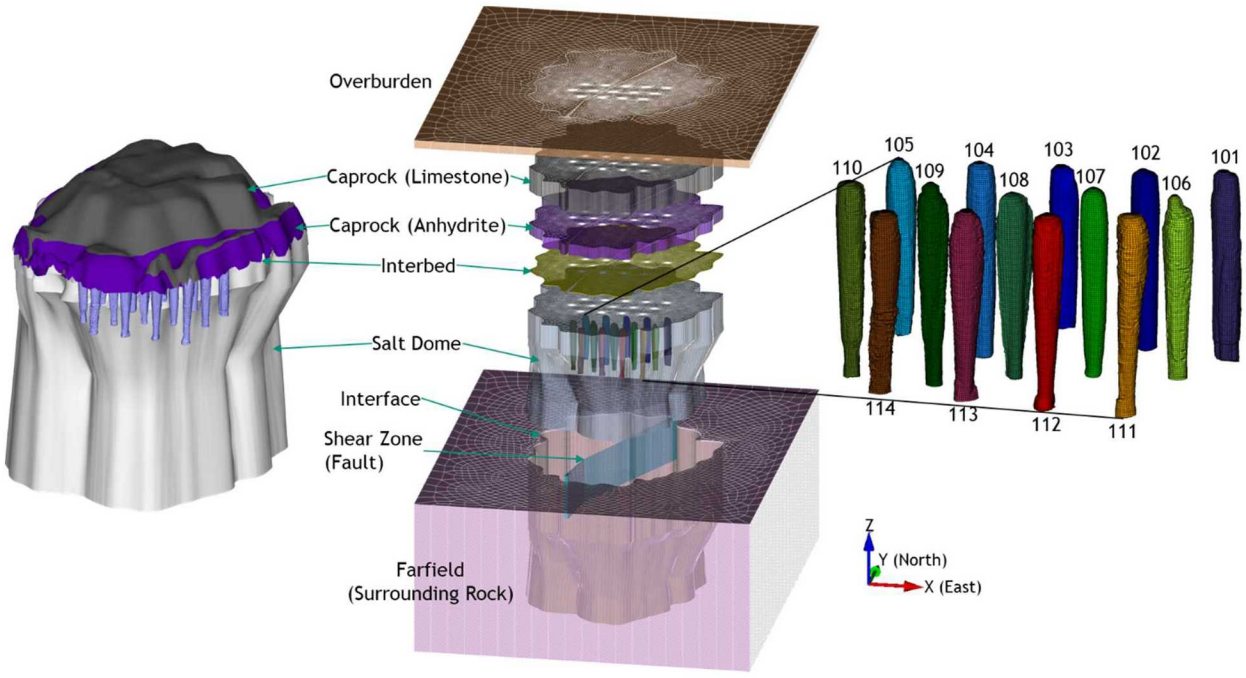

Figure 3. Images of Big Hill salt dome and caprock obtained from the seismic, sonar and borehole survey (left), an overview of the meshes of the stratigraphy (middle), and caverns (right). The cavern ID numbers are also shown [Park, 2017a].

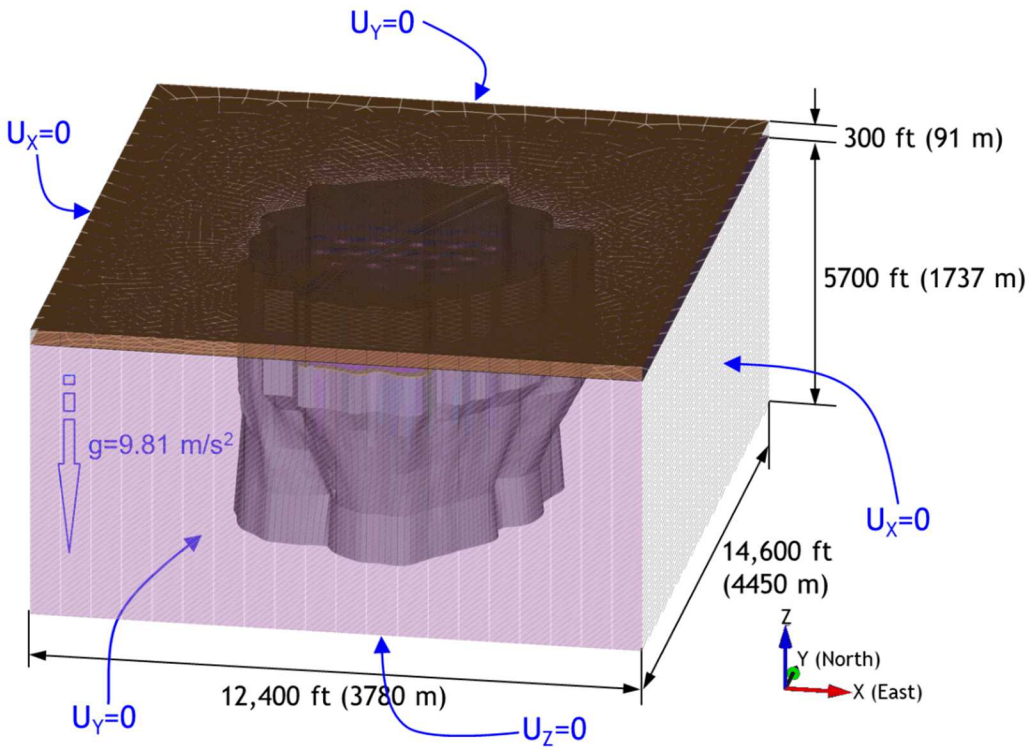

Figure 4. Entire finite element model and boundary conditions at Big Hill. U_x=0, U_Y=0, and U_Z=0 means no displacement in X, Y, and Z-directions, respectively, at every node [Park, 2017a].

3.2. Internal Pressure Change

The modeling simulates the cavern responses forward in time from the initial cavern creation. The actual wellhead pressure histories of BH-101 through BH-114 have been recorded since the dates in Table 1 as shown Figure 5. They are recorded at the oil-side wellhead, i.e. oil-side wellhead pressure. Pressure drops occurred during workovers and fluid transfers. For the purposes of the present simulation, it is assumed that the initial leaches of the caverns started on dates one year before the wellhead pressure recording started, i.e. they were leached to full size over a one-year period. For example, the wellhead pressure of BH-101 was recorded from 9/19/1990, so it is assumed that the initial leach of BH-101 started on 9/19/1989 with one year leaching period.

Figure 6 shows the wellhead histories, which consist of the actual (4/20/1990 - 9/18/2017) and the assumed future (9/19/2017 - 9/18/2047) pressure records used for each of the 14 SPR caverns in the simulation. The previous approximately two-year (2/3/2007 - 2/12/2009) wellhead pressure history of each cavern as shown in Figure 5 is selected for the assumed future wellhead pressure replication. The selected period, during which no drawdowns take place, contains the typical normal operation histories. These histories are replicated two and half times for the next five-years (9/19/2017 - 9/18/2022). This five-year histories are replicated for the next five-year drawdown cycles thereafter (9/19/2022 - 9/18/2047). The first drawdown leach is assumed to start at

9/19/2022. Note that the 1st, 2nd, etc., in the plots indicate the drawdown leach start dates (9/19/2022, 9/19/2027, 9/19/2032, 9/19/2037, and 9/19/2042, respectively).

In general, the SPR caverns are most susceptible to structural instability when a workover is in progress. In this analysis, the workover is simulated by means of an internal pressure change in the SPR caverns. Modeling of the workover processes is used to investigate the structural stability of the caverns. For simulation purposes, the pressure drop to zero psi for each cavern lasts for three months, or 5 percent of time during a 5-year period. The duration of the workover may be slightly longer than is historically encountered in the field, but is chosen to provide an adverse condition and closely simulate actual subsidence measurements [Park et al. 2005].

Rather than complicating the analyses, the following assumptions are made:

- The replicated five-year histories (9/19/2017 - 9/18/2022) are applied for the future simulation, with pressure drops periodically included.
- For workover conditions, zero wellhead pressure is used.
- Not all caverns are in workover mode at the same time.
- BH-101 is the first cavern in the workover which starts on 1/1/2019 and lasts for three months.
- After that, workovers are performed on BH-102, BH-103 …, and BH-114 in order with three months duration as shown Figure 6.
- These workover cycles are repeated every 5 years to meet the drawdown cycles.
- The pressure due to the oil and brine in the cavern plus the wellhead is applied on the cavern inside boundary.

Before a cavern's initial leach starts, the model has a stabilization period (1/1/1900 - 4/20/1989). To avoid the numerical shock, gravity is applied gradually into the mesh for ten seconds. After that, the model is allowed to consolidate with gravity for approximately 89 years so that every element is stabilized numerically.

The analysis simulates caverns that were leached to full size over a one-year period by means of gradually switching from salt to fresh water in the caverns. Creep is permitted to occur over the entire simulation period (1/1/1900 - 9/18/2047). On 9/19/2022 and subsequently every 5 years thereafter, the SPR caverns are instantaneously leached to produce an increased volume of 16% during each leach cycle to simulate drawdowns. The 5-year period between each drawdown allows the stress state in the salt to return to a steady-state condition, as will be evidenced in the predicted closure rates. The simulation was run out to 9/18/2047 to investigate the structural behavior of the dome for approximately 57 years, as the process of salt creep continues to reduce the caverns' volume.

In actuality, the caverns were not always fully filled with just oil. Brine fills the bottom of the caverns, and the proportion changes with time depending on cavern operations. The difference between pressure gradients of oil (0.37 psi/ft of depth) and brine (0.52 psi/ft of depth) cannot be ignored [Park, 2017a]. So, the amount of oil and brine in a cavern over time needs to be considered. Figure 7 shows the oil-brine interface (OBI) depth history of SPR caverns used in this analysis. The history data (1/1/1990– 9/18/2017) were obtained from the BH field office. The previous approximately two-year (2/3/2007 - 2/12/2009) OBI history of each cavern is selected for the assumed future OBI replication for the rest of the simulation.

As far as withdrawing oil, they keep the pressure between 400 and 500 psi during the transfer, typically, and it stays that way as long as they are pumping. The maximum drawdown rate is 12 Mbbl/hour, i.e. 288 Mbbl/day. However, they never withdraw at that rate. In general, they typically remove around 100 Mbbl per day for 10 to 18 hours. So the OBI change is going to be dependent on the strapping curve and shape of the cavern. A daily pressure during a drawdown would be about 400 psi (oil-side wellhead) for three days before the transfer, the same throughout the drawdown period, then jumping back up operational range at the end [Hart, 2019].

The following assumptions are made for the future OBI histories (9/19/2017-9/18/2047):

- The duration of withdrawing oil is 4 months, because 14 cavern volumes range 14.2 MMB (BH101) to 11.2 MMB (BH108) [Park, 2019b], and 0.1 MMB/day is assumed for the oil withdrawing rate. The same duration is applied to all 14 caverns for the simplification (Figure 7).
- Each cavern is emptied completely after the withdrawal period, and then filled with oil again for two years – The OBI moves up from the cavern bottom, which is actually obtained from the OBI replication period for the normal operation (2/3/2007 - 2/12/2009), to top for four months, and then moves down from the cavern top to bottom for two years.
- The wellhead pressure drops from the normal operation pressure of each cavern to 400 psi for three days and is kept at 400 psi during the withdrawal of oil for four months and then returns to the normal operation pressure for three days (Figure 6).
- The replicated five-year histories of OBI (5/19/2022 - 5/18/2027) are applied for the future OBI histories and these withdrawing cycles are repeated every five years.
- All caverns are in withdrawal mode at the same time.
- The pressure due to the oil and brine in the cavern plus the wellhead is applied on the cavern inside boundary.

Table 1. Dates of initial leach completion, wellhead pressure recording started, and assumed initial leach started

Cavern ID	Date of Initial Leach Completion	Date of Wellhead Pressure Recording Started	Assumed Date Initial Leach Started
BH-101	09/17/1990	09/19/1990	09/19/1989
BH-102	10/19/1990	10/20/1990	10/20/1989
BH-103	11/27/1990	11/29/1990	11/29/1989
BH-104	10/21/1990	10/21/1990	10/21/1989
BH-105	05/13/1990	05/14/1990	05/14/1989
BH-106	10/15/1990	10/17/1990	10/17/1989
BH-107	04/23/1990	04/25/1990	04/25/1989
BH-108	06/13/1990	06/14/1990	06/14/1989
BH-109	07/23/1990	07/25/1990	07/25/1989
BH-110	04/18/1990	04/20/1990	04/20/1989
BH-111	07/14/1991	07/15/1991	07/15/1990
BH-112	06/17/1991	06/19/1991	06/19/1990
BH-113	04/30/1991	05/02/1991	05/02/1990

BH-114	08/26/1991	08/29/1991	08/29/1990

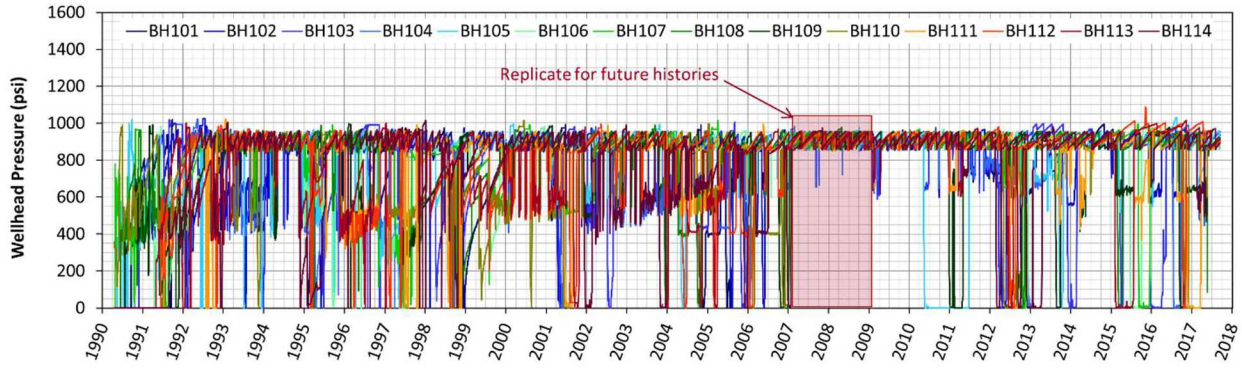

Figure 5. Field wellhead pressure histories for the 14 Big Hill SPR caverns

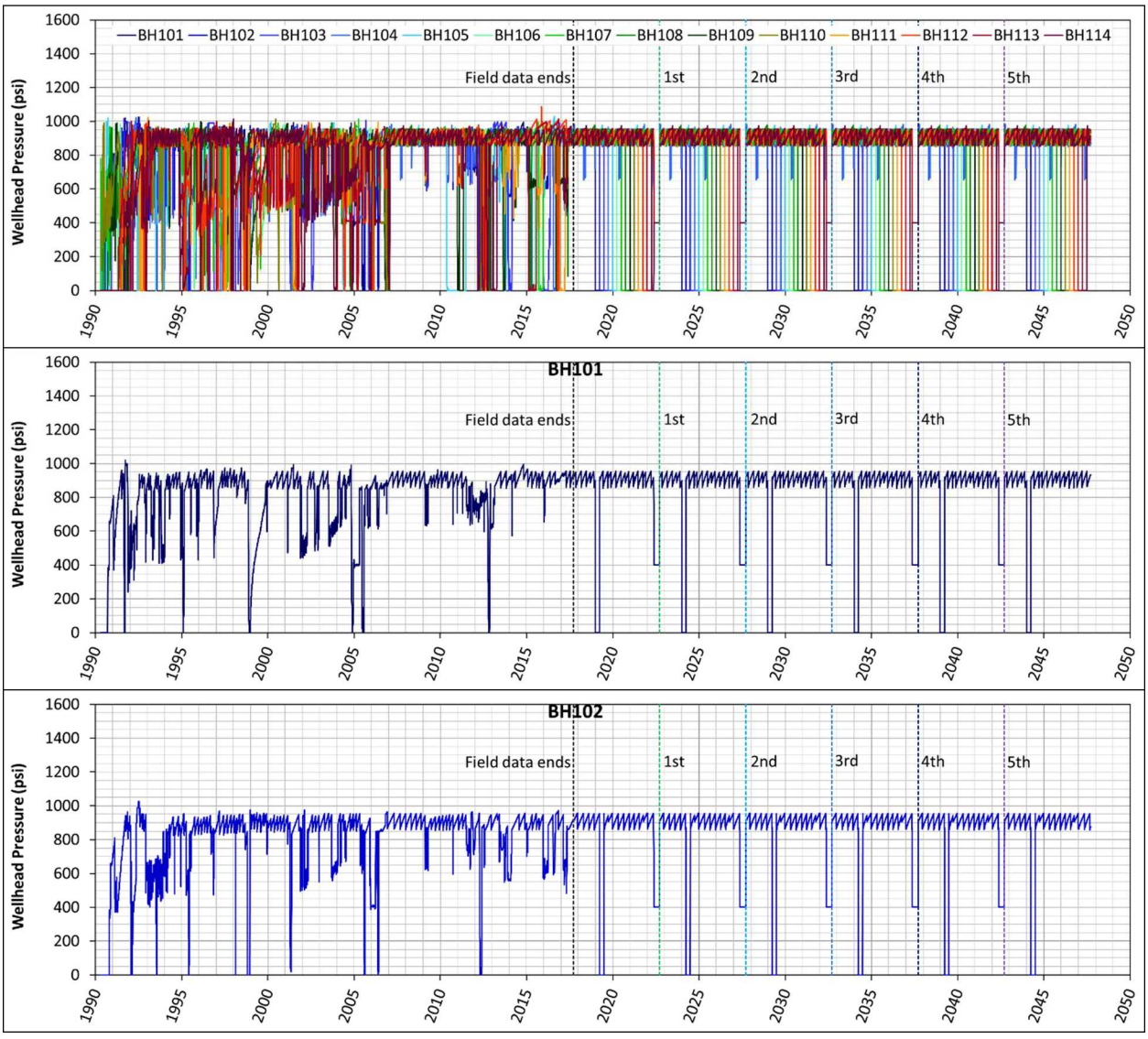

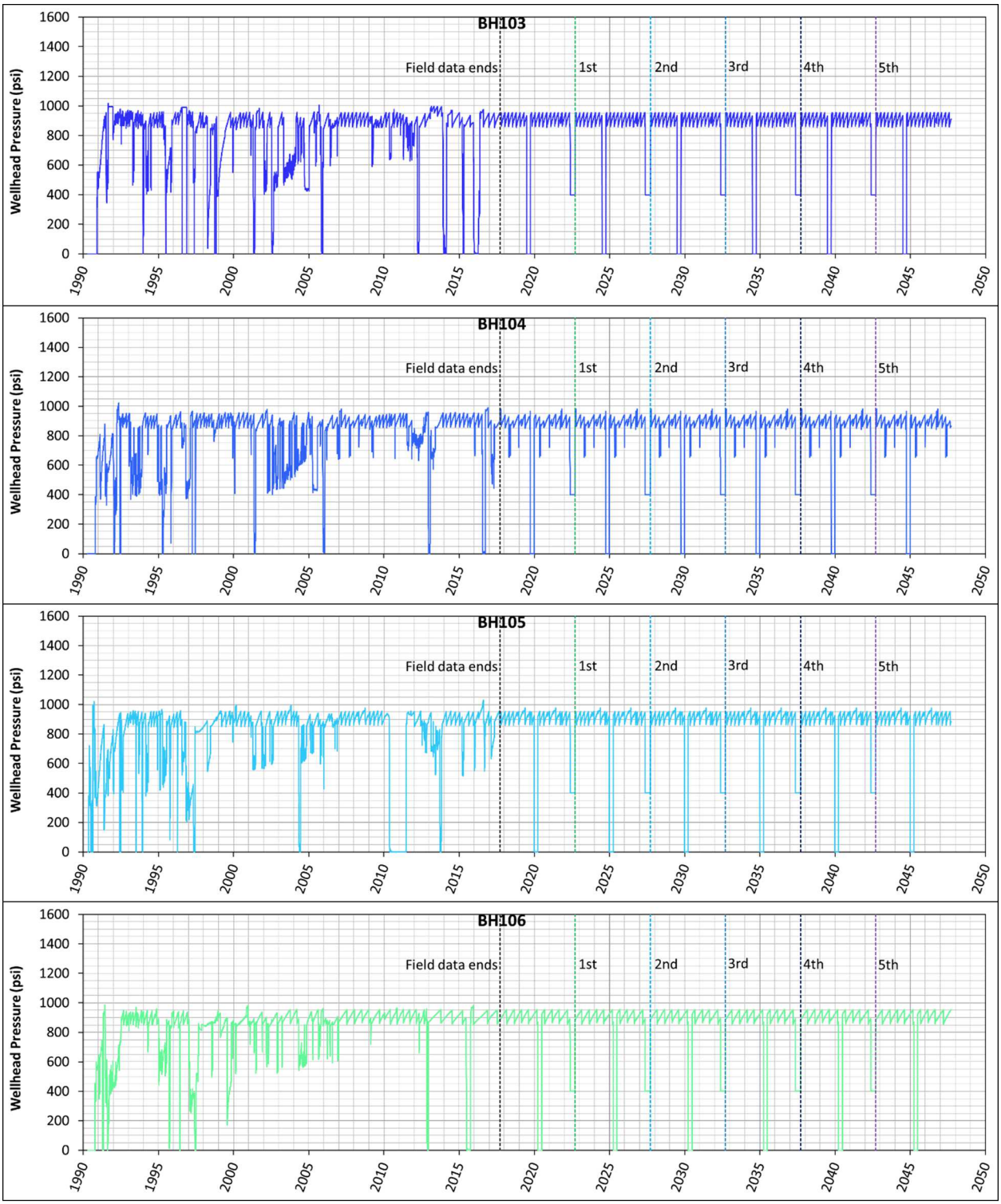
BH103
BH104
BH105
BH106
Field data ends
1st
2nd
3rd
4th
5th
Wellhead Pressure (psi)
0
200
400
600
800
1000
1200
1400
1600
1990
1995
2000
2005
2010
2015
2020
2025
2030
2035
2040
2045
2050

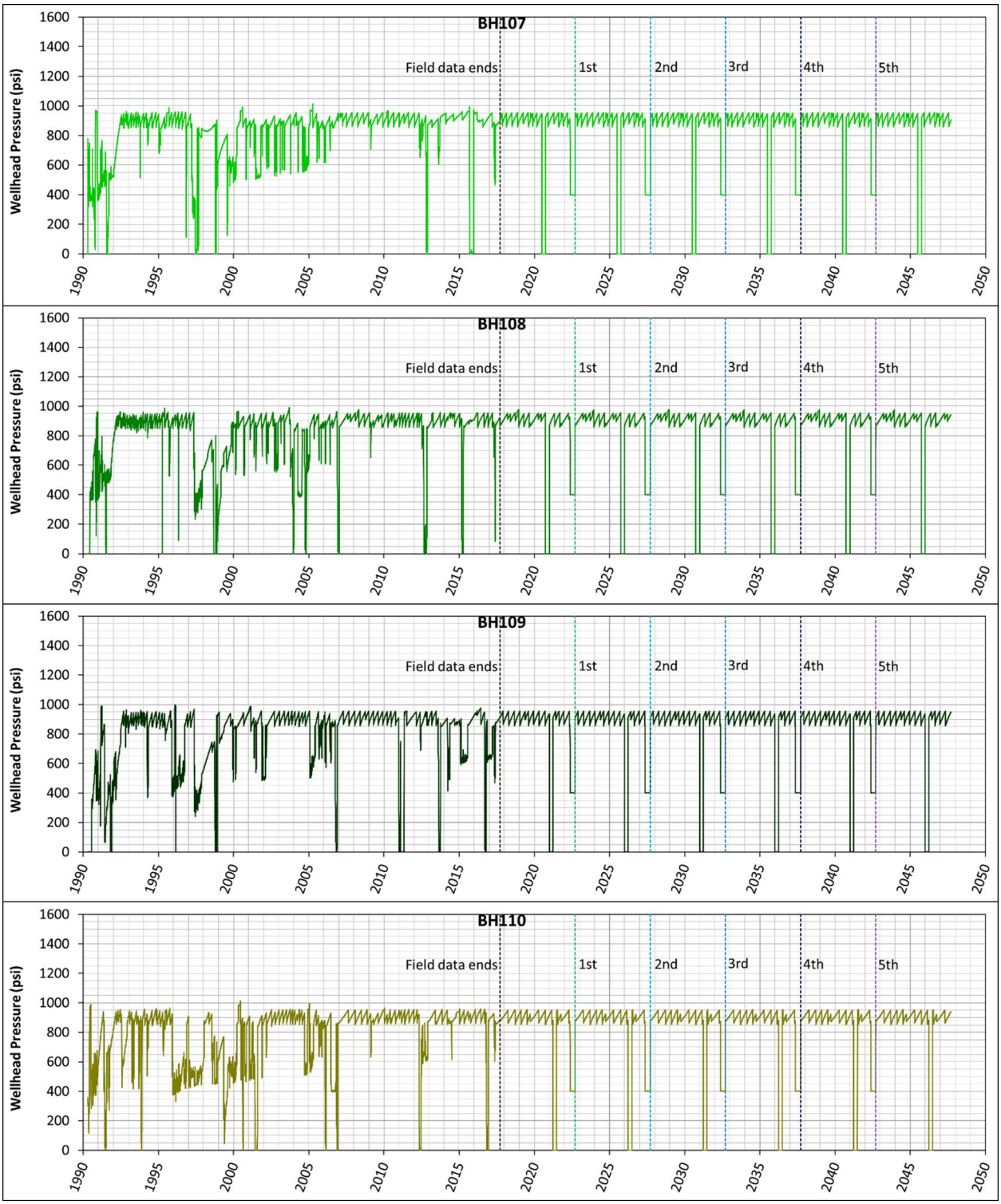
BH107
Field data ends
1st
2nd
3rd
4th
5th
Wellhead Pressure (psi)
0
200
400
600
800
1000
1200
1400
1600
1990
1995
2000
2005
2010
2015
2020
2025
2030
2035
2040
2045
2050
BH108
Field data ends
1st
2nd
3rd
4th
5th
Wellhead Pressure (psi)
BH109
Field data ends
1st
2nd
3rd
4th
5th
Wellhead Pressure (psi)
BH110
Field data ends
1st
2nd
3rd
4th
5th
Wellhead Pressure (psi)

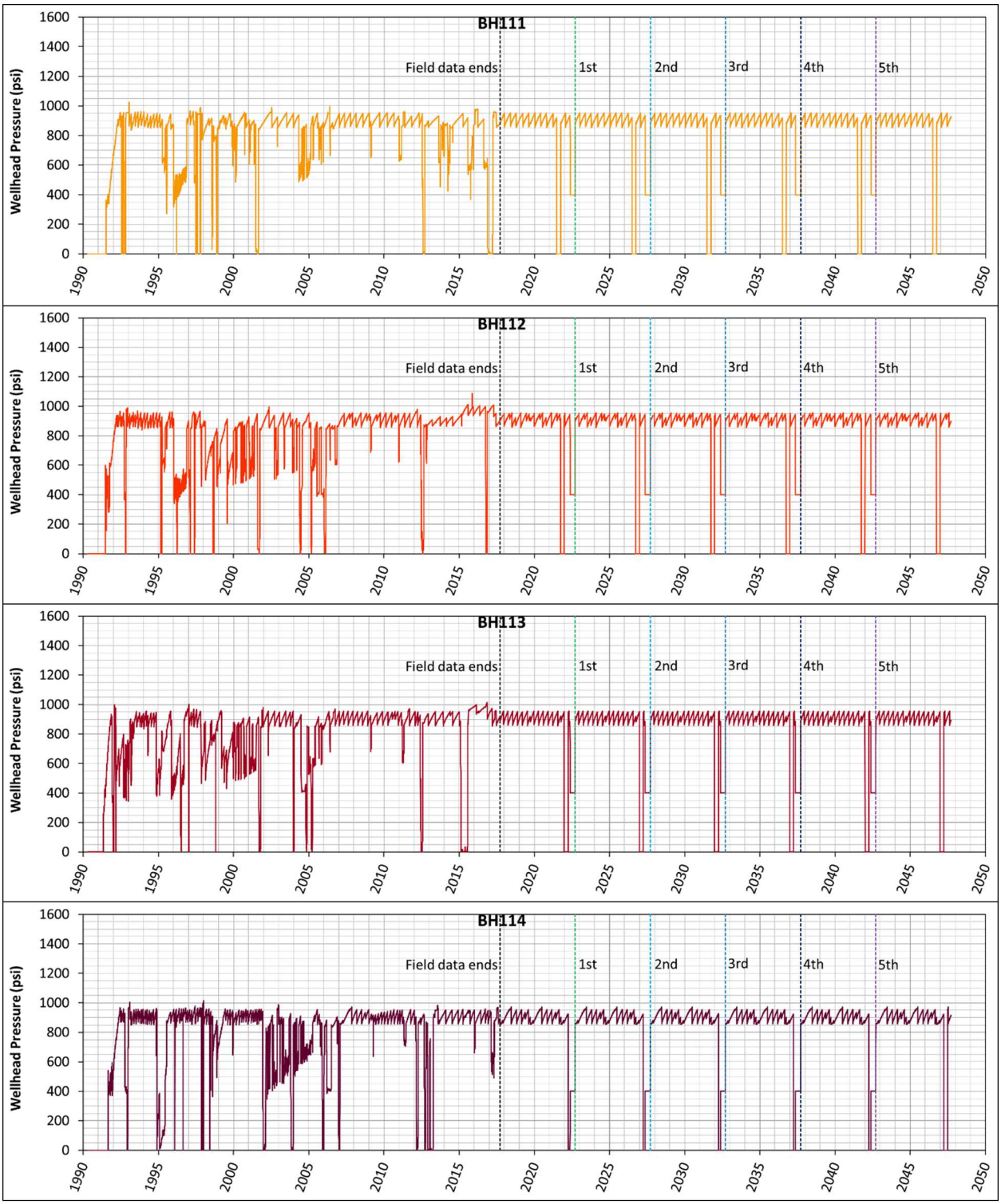

Figure 6. Individual Big Hill SPR caverns' wellhead pressure histories used in this analysis

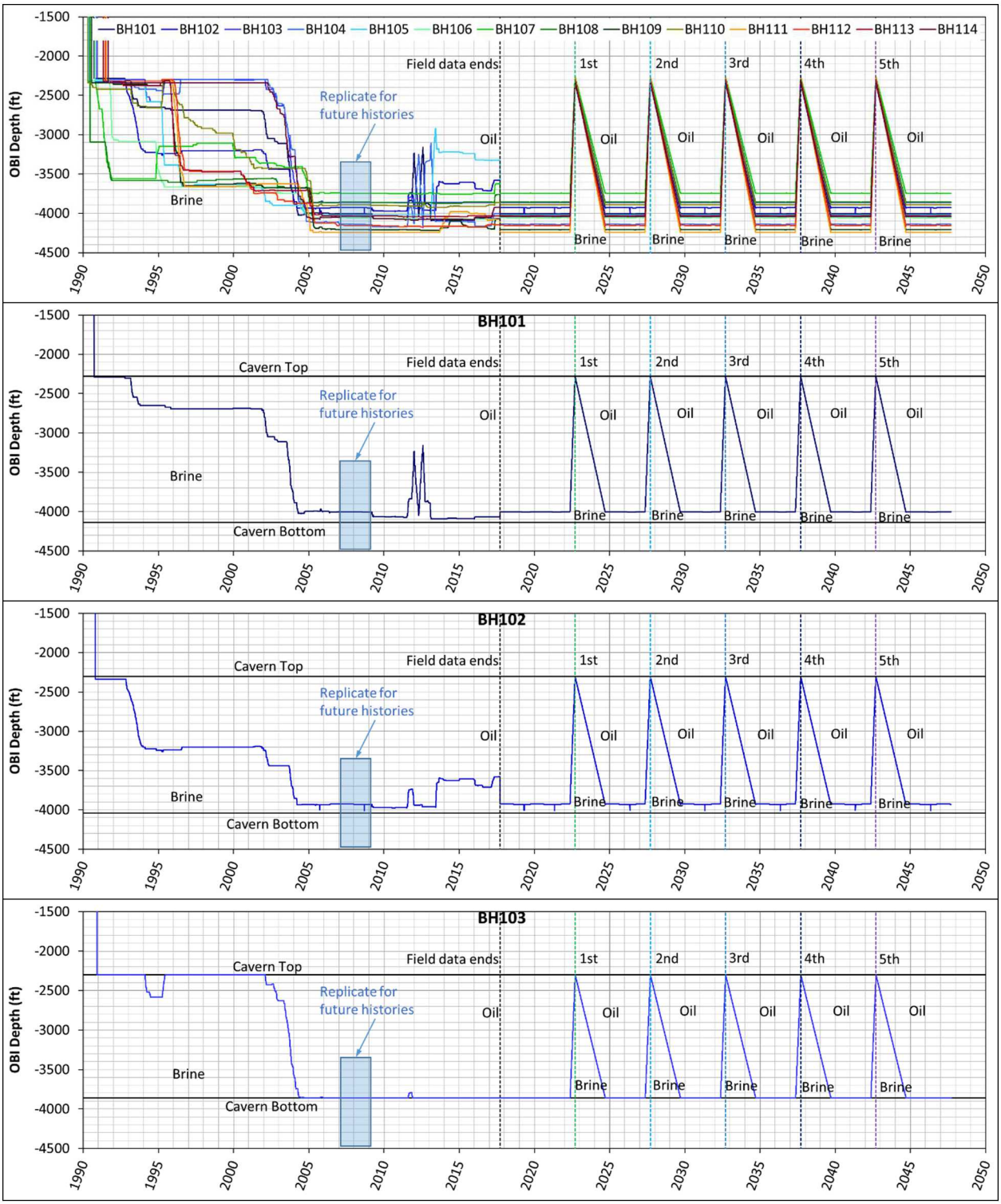
BH101 BH102 BH103 BH104 BH105 BH106 BH107 BH108 BH109 BH110 BH111 BH112 BH113 BH114
OBI Depth (ft)
-1500
-2000
-2500
-3000
-3500
-4000
-4500
1990
1995
2000
2005
2010
2015
2020
2025
2030
2035
2040
2045
2050
Field data ends
1st
2nd
3rd
4th
5th
Replicate for future histories
Oil
Brine
BH101
Cavern Top
Cavern Bottom
BH102
BH103

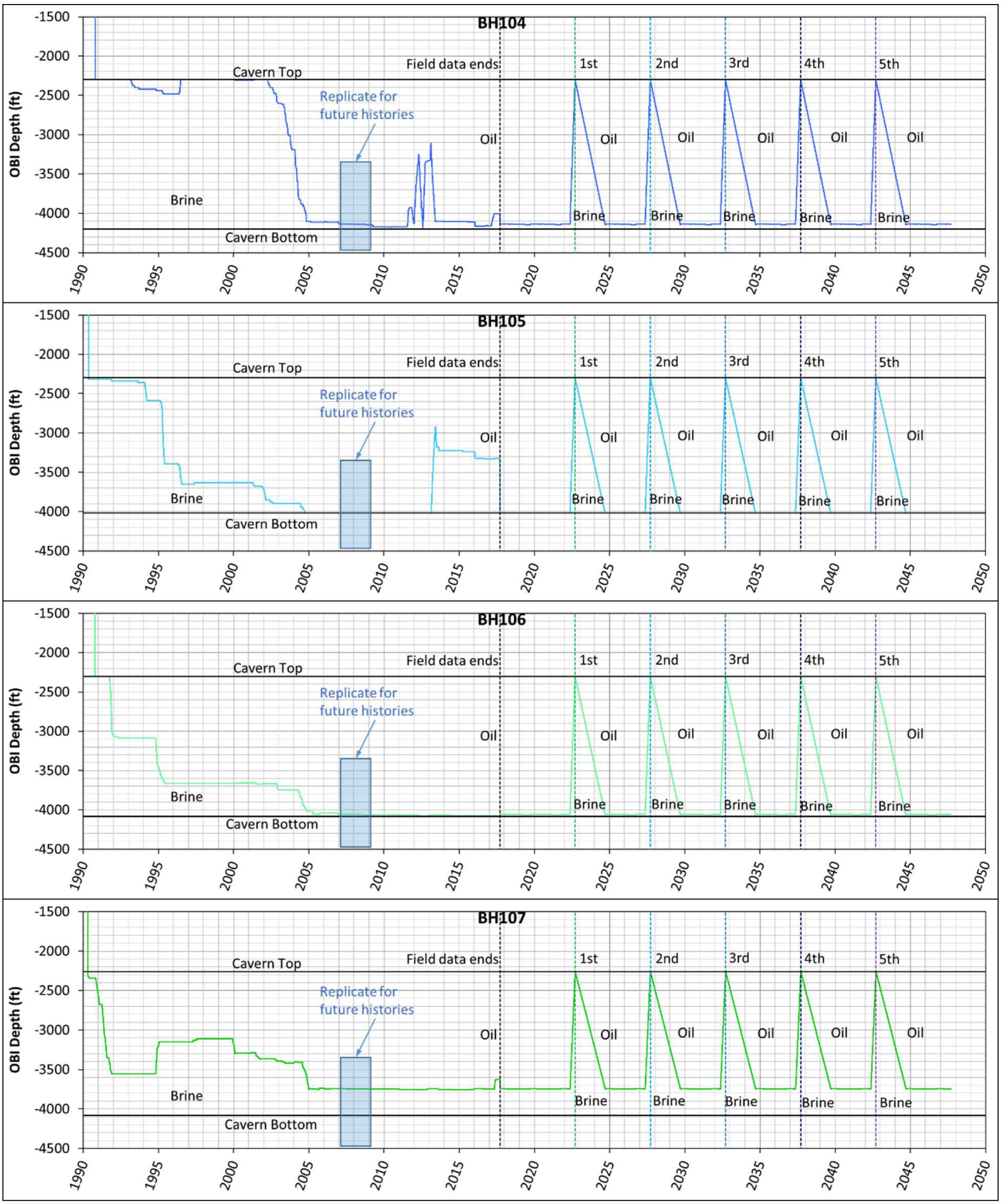
BH104
BH105
BH106
BH107
OBI Depth (ft)
-1500
-2000
-2500
-3000
-3500
-4000
-4500
1990
1995
2000
2005
2010
2015
2020
2025
2030
2035
2040
2045
2050
Cavern Top
Cavern Bottom
Field data ends
Replicate for future histories
1st
2nd
3rd
4th
5th
Oil
Brine

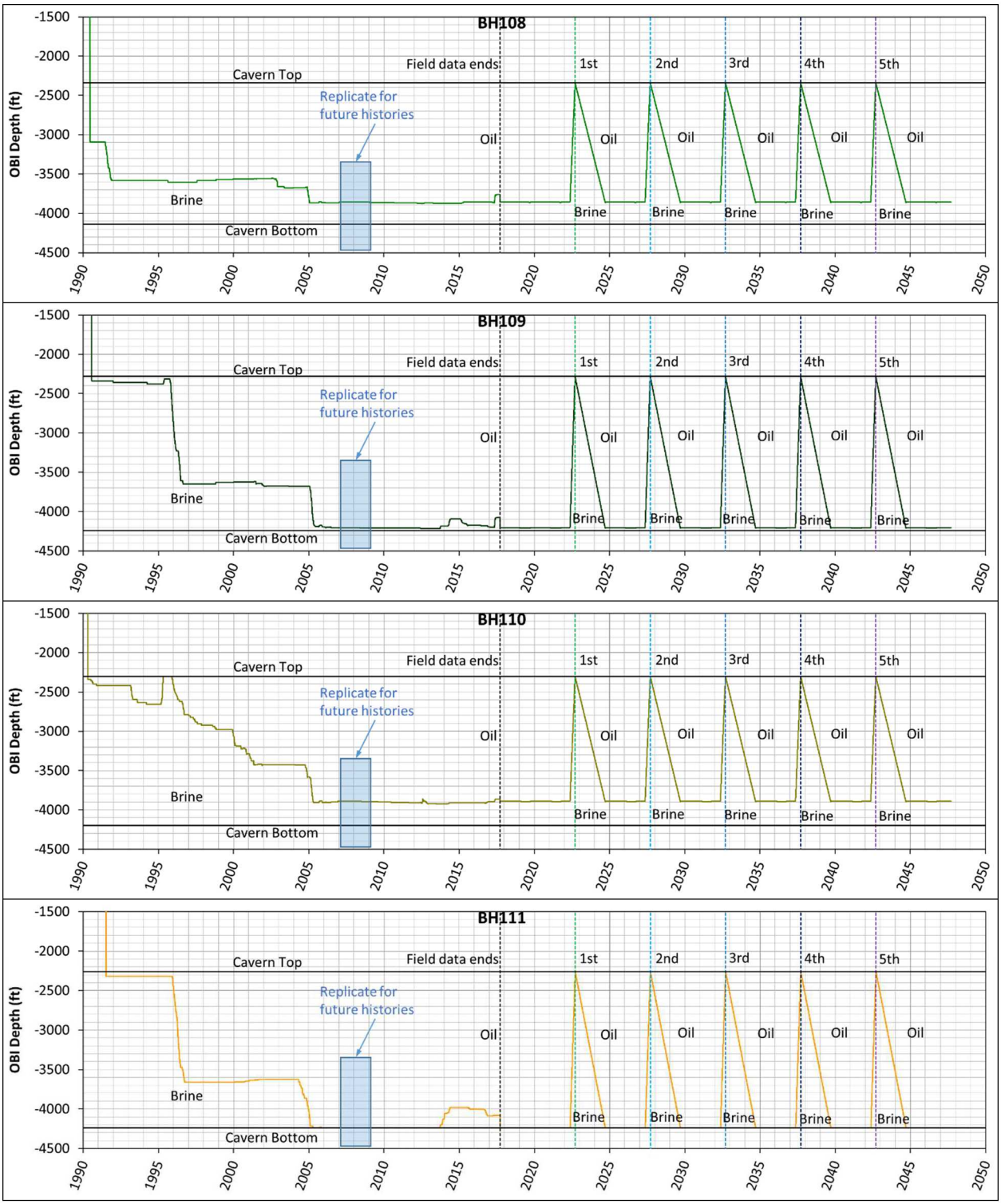
BH108
BH109
BH110
BH111
OBI Depth (ft)
-1500
-2000
-2500
-3000
-3500
-4000
-4500
1990
1995
2000
2005
2010
2015
2020
2025
2030
2035
2040
2045
2050
Cavern Top
Cavern Bottom
Field data ends
Replicate for future histories
1st
2nd
3rd
4th
5th
Oil
Brine

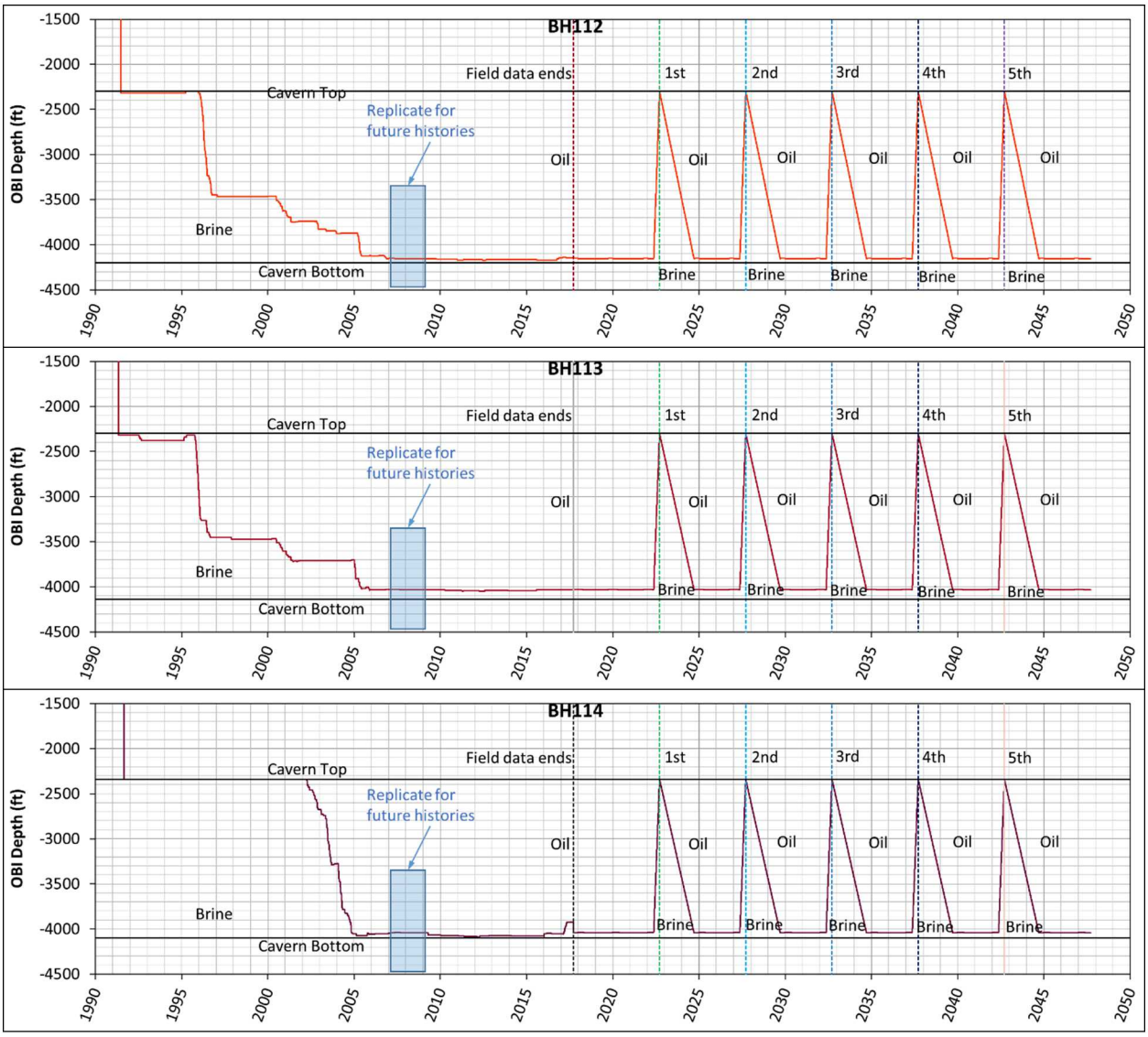

Figure 7. Oil-Brine Interface depth histories applied to the simulations for the 14 Big Hill SPR caverns

4. SALT DAMAGE CRITERIA

Potential damage to or around the SPR caverns was evaluated based on two failure criteria: dilatant damage and tensile failure.

For purpose of these analyses, the tensile strength of the salt is conservatively assumed to be zero in order to check for tensile failure. Tensile cracking in rock salt initiates perpendicular to the largest tensile stress direction. The potential for tensile failure exists if the maximum principal stress (σ_1) is numerically zero or tensile (a positive value of σ_1).

Dilatancy is attributed to micro-fracturing or changes in the pore structure of the salt, resulting in an increase in permeability. A dilatancy is considered as the onset of damage to rock salt. A dilatant damage criterion is used to delineate potential zones of damage in the salt formation surrounding the SPR facility. Dilatant damage criterion typically relates two stress invariants to access failure and/or dilation of pressure-dependent materials: the first invariant of the Cauchy stress tensor, I_1, and the second invariant of the deviatoric stress tensor, J_2. These two invariants are defined mathematically as:

$$I_1 = \sigma_1 + \sigma_2 + \sigma_3 \tag{1}$$

$$J_2 = \frac{(\sigma_1 - \sigma_2)^2 + (\sigma_2 - \sigma_3)^2 + (\sigma_3 - \sigma_1)^2}{6} \tag{2}$$

where, σ_1, σ_2, and σ_3 are the maximum, intermediate, and minimum principal stresses, respectively. Lee et al. [2004] suggested the following strength criterion of BH salt based on a series of quasi-static triaxial compression tests:

$$\sqrt{J_2} = a \cdot e^{n \cdot I_1} + c \tag{3}$$

The values of the parameters are calculated as follows:

a = -1320.5 psi
n = -3.4 × 10^{-4} (1/psi)
c = 1746 psi

A dilatant damage factor (*DF*) for the BH salt can then be defined by:

$$DF = \frac{a \cdot e^{n \cdot I_1} + c}{\sqrt{J_2}} \tag{4}$$

If $DF \leq 1$, the shear stresses in the salt ($\sqrt{J_2}$) are large compared to the mean stress (I_1) and dilatant behavior is expected. If $DF > 1$, the shear stresses are small compared to the mean stress and dilatant damage is not expected. To calculate the dilatancy damage potential in salt, the post-processing code ALGEBRA is used with the output of the FE code ADAGIO to determine spatial locations of dilatant damage.

This page left blank

5. CAVERN INTEGRITY

5.1. BH-101

Modeling of the leaching process of the caverns is performed by deleting a pre-meshed block of elements along the walls of the cavern so that the cavern volume is increased by 16 percent per drawdown. The exact volume increase depends on the insoluble content of salt, so a 16% volume increase is used for a drawdown for the BH salt [Park et al. 2005; Park and Ehgartner, 2011]. Also, typical leaching processes tend to increase a cavern's radius more at the bottom than at the top of the cavern, with very little change to the roof and floor. For the purposes of this modeling effort for Big Hill, leaching is assumed to add 16% to the volume of the cavern, and is assumed to occur uniformly along the entire height of the cavern, with no leaching in the floor or roof of the caverns. Each leaching layer, or "onion skin," is built around the perimeter of the meshed cavern volume using the same rules stated previously.

Figure 8 shows the cavity of BH-101 as developed from sonar data, along with drawdown skins (leaching layers) and extra skins. In this simulation, BH-101 is modeled as having five drawdown layers to be removed to account for the future oil drawdown activities. The thicknesses of five layers and extra skin 1 are calculated to get a 16% cavern volume increase for each drawdown. Five drawdown skins and extra skin 1 are used for examining the analysis results after the initial leach, 1st drawdown, 2nd drawdown, … and 5th drawdown leaches, respectively. Six layers and an extra skin 2 of 40 ft thickness are used for applying the cavern specific calibrated values of multiplication factors, *A2F* and *K0F* [Park, 2017a].

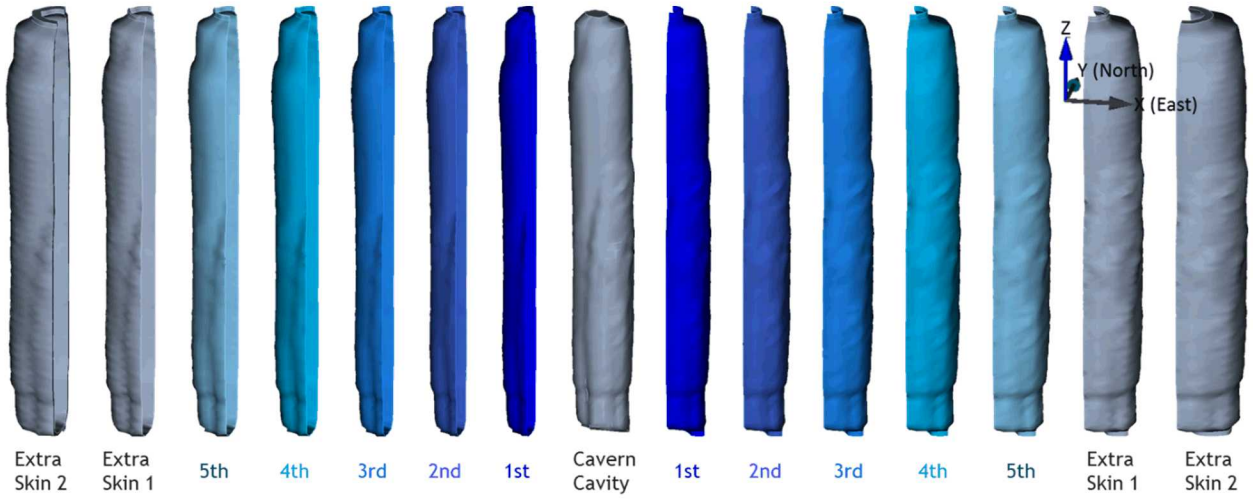

Figure 8. BH-101 cavern cavity with five drawdown skins (leaching layers) and extra skins

Figure 9 shows the predicted volumetric change (top), and volumetric closure normalized to initial cavern volume (2nd panel), maximum σ_1 (3rd panel), and minimum *DF* (bottom) in the salt volume surrounding BH-101. In the numerical analysis, σ_1 is calculated in every element in the salt dome at each time step. The maximum σ_1 means the maximum value among all σ_1 values calculated in all elements in a specific volume (in this case, each skin layer) at a specific time. In the plot, a positive value (+) indicates a tensile stress. In the similar manner, *DF* is calculated in every element in the salt

dome at each time step. The minimum *DF* means the minimum value among all *DF* values calculated in all elements in a specific volume at a specific time. As mentioned in Section 4, when $DF \leq 1$, we consider dilatant damage to have occurred. Note that the 1st, 2nd, etc., in the plots indicate the drawdown leach start dates (9/19/2022, 9/19/2027, 9/19/2032, 9/19/2037, and 9/19/2042, respectively) of all SPR caverns.

The initial cavern cavity volume was 13.1 MMB on 9/20/1990 and is predicted to be 11.9 MMB on 8/20/2022. The cavern volume is predicted to decrease by 8.8% over 32 years (9/20/1990 - 8/20/2022).

The maximum σ_1 reaches a positive (tensile stress state) value during the workovers after the fourth drawdown leach. The maximum σ_1 are calculated to be 45 psi at 2039.22 years (on 3/21/2039). Figure 10 shows the contour plots of σ_1 on 3/21/2039 to show the area in tension in the cavern skin layers during the workovers after the 4th drawdown leach. The areas in tensile state are located in the sloping floor. The tensile state may occur because of the geometry of the relatively horizontal floor, but not vertical wall.

The minimum *DF* never reaches to be less than 1 during every workover until the end of simulation. The smallest predicted value of the minimum *DF* is 1.15 on 3/21/2039.

In conclusion, BH-101 is expected to be structurally stable until the fifth drawdown leach. However, the tensile stressed area is created on the sloping floor of the cavern during the workovers after the 4th drawdown leach substantially. The consequences of a salt fracture here are minimal, in that it is unlikely to propagate to a nearby cavern, and it is in the brine-filled portion of the cavern. In addition, because the predicted tensile stress is confined to a small area at the bottom of the cavern where the sonar measurements of geometry gives a more jagged surface, the predicted tensile stress may be more of a numerical artifact than a true tensile condition. However, tensile stresses are something ideally to be avoided. Therefore, we recommend a re-examination of the cavern stability with a new cavern volume obtained from a sonar after a drawdown leach in future.

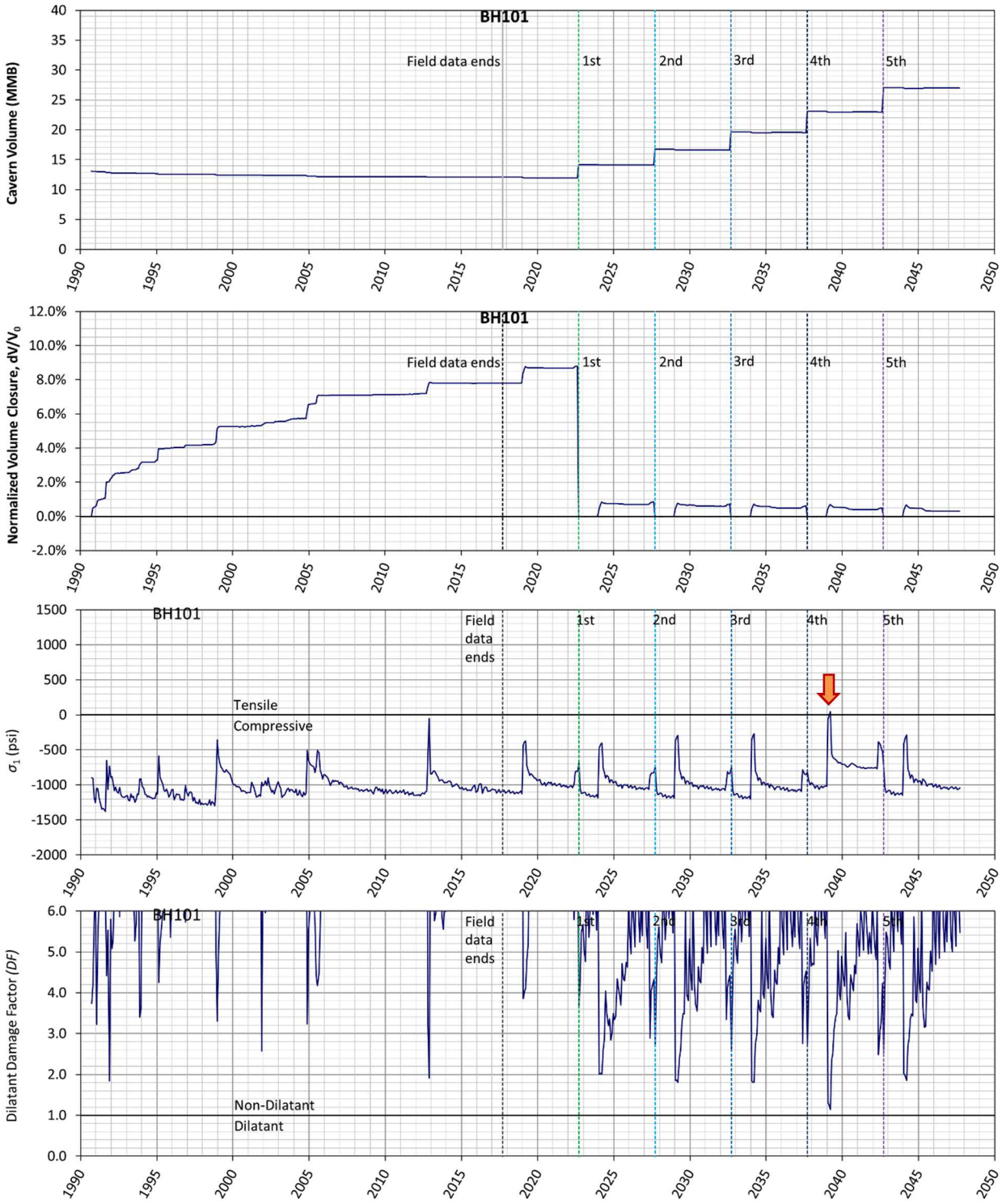

Figure 9. Predicted volumetric change (top), volumetric closure normalized to initial cavern volume of BH-101 (2nd), maximum σ_1 (3rd) and minimum dilatant damage factor (bottom) in the salt surrounding BH-101 over time

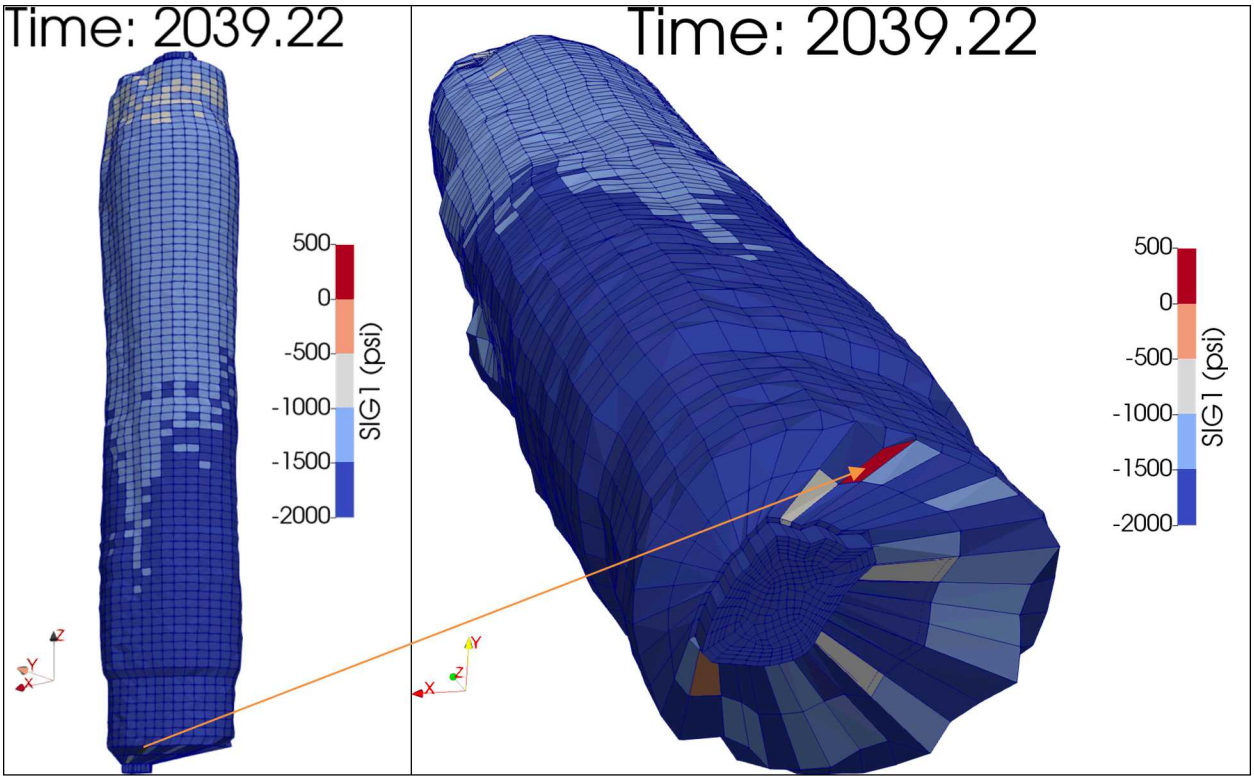

Figure 10. Contour plots of σ_1 on 2039.22 (3/21/2039). Areas in tensile state are shown in red ($\sigma_1 > 0$). The value of maximum σ_1 are indicated by the arrow on 3/21/2039 in the 3rd panel in Figure 9

5.2. BH-102

Modeling of the leaching process of the caverns is performed by deleting a pre-meshed block of elements along the walls of the cavern so that the cavern volume is increased by 16 percent per drawdown. Figure 11 shows the cavity of BH-102 as developed from sonar data, along with drawdown skins and extra skins. In this simulation, BH-102 is modeled as having five drawdown layers to be removed to account for the future oil drawdown activities as mentioned in the previous section.

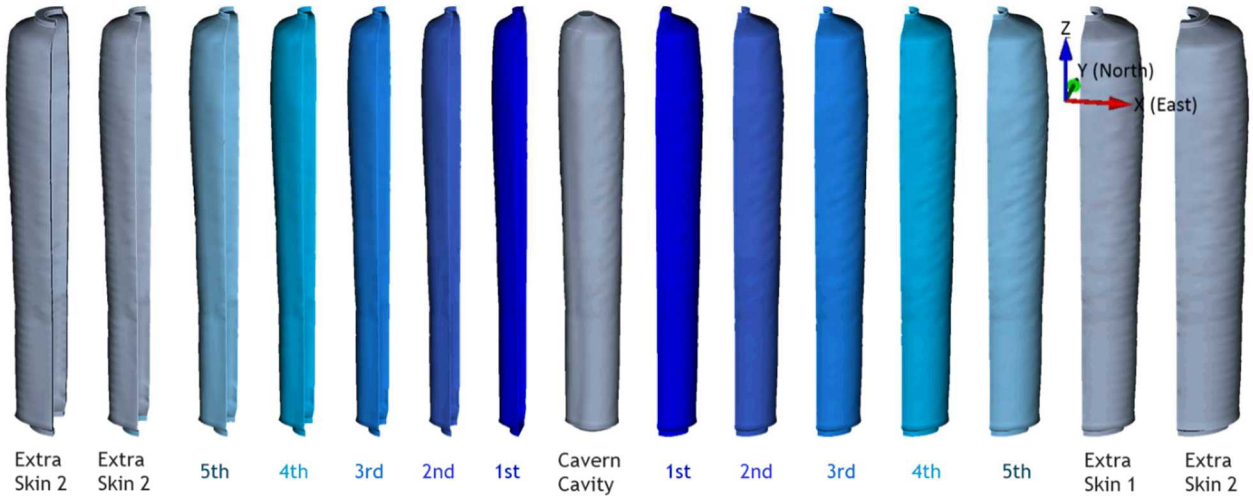

Figure 11. BH-102 cavern cavity with five drawdown skins (leaching layers) and extra skins

Figure 12 shows the predicted volumetric change (top), and volumetric closure normalized to initial cavern volume (2nd panel), maximum σ_1 (3rd panel), and minimum *DF* (bottom) in the salt volume surrounding BH-102 over time. The initial cavern cavity volume was 12.9 MMB on 10/20/1990 and is predicted to be 12.0 MMB on 8/20/2022. The cavern volume is predicted to decrease by 7.3% over 32 years (10/20/1990 - 8/20/2022).

The maximum σ_1 never reaches a positive (tensile stress state) value through five drawdowns, and the minimum *DF* either never reaches to be less than 1 during every workover until the end of simulation. The largest predicted value of the maximum σ_1 is -515 psi on 6/21/2019 during the workover started on 4/1/2019 for 90 days. The smallest predicted value of the minimum *DF* is 1.88 on 8/20/2005 during the workover started on 7/20/2005 for 31 days.

In conclusion, BH-102 is predicted to be structurally stable through the fifth drawdown leach.

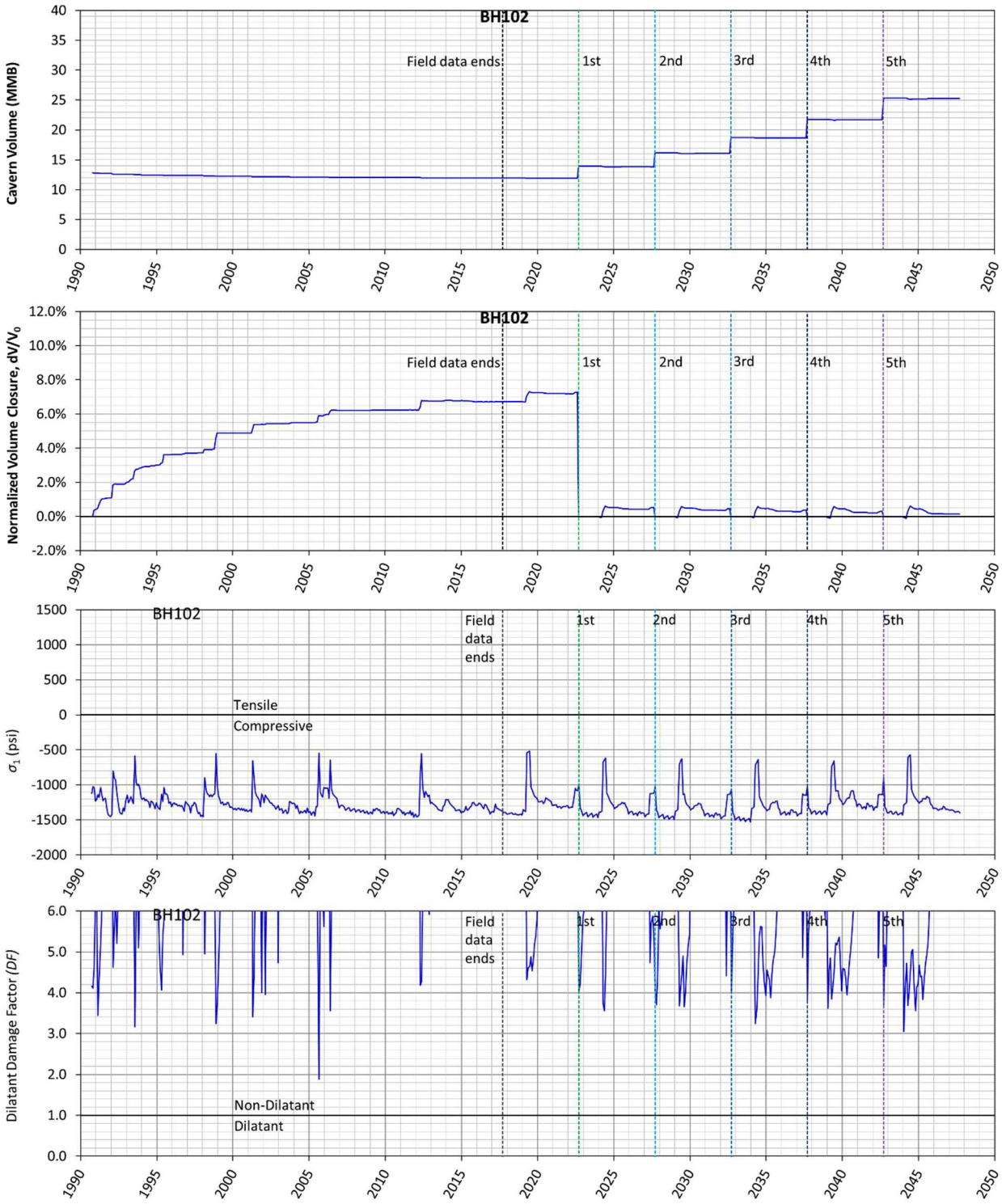

Figure 12. Predicted volumetric change (top), volumetric closure normalized to initial cavern volume of BH-102 (2nd), maximum σ_1 (3rd) and minimum dilatant damage factor (bottom) in the salt surrounding BH-102 over time

5.3. BH-103

Modeling of the leaching process of the caverns is performed by deleting a pre-meshed block of elements along the walls of the cavern so that the cavern volume is increased by 16 percent per drawdown. Figure 13 shows the cavity of BH-103 as developed from sonar data, along with drawdown skins and extra skins. In this simulation, BH-103 is modeled as having five drawdown layers to be removed to account for the future oil drawdown activities.

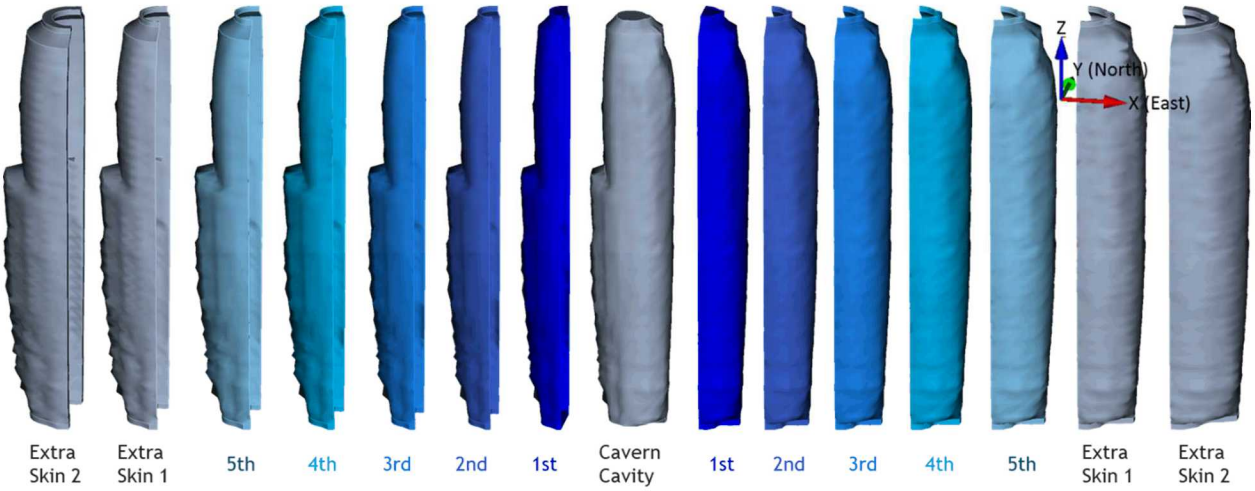

Figure 13. BH-103 cavern cavity with five drawdown skins (leaching layers) and extra skins

Figure 14 shows the predicted volumetric change (top), and volumetric closure normalized to initial cavern volume (2nd panel), maximum σ_1 (3rd panel), and minimum *DF* (bottom) in the salt volume surrounding BH-103 over time. The initial cavern cavity volume was 13.0 MMB on 11/20/1990 and is predicted to be 12.1 MMB on 8/20/2022. The cavern volume is predicted to decrease by 6.9% over 32 years (11/20/1990 - 8/20/2022).

The maximum σ_1 never reaches a positive (tensile stress state) value through five drawdowns, and the minimum *DF* either never reaches to be less than 1 during every workover until the end of simulation. The largest predicted value of the maximum σ_1 is -141 psi on 9/20/2044 during the workover started on 7/1/2044 for three months. The smallest predicted value of the minimum *DF* is 2.41 on 7/20/2044 during the workover started on 7/1/2044 for three months.

In conclusion, BH-103 is predicted to be structurally stable through the fifth drawdown leach.

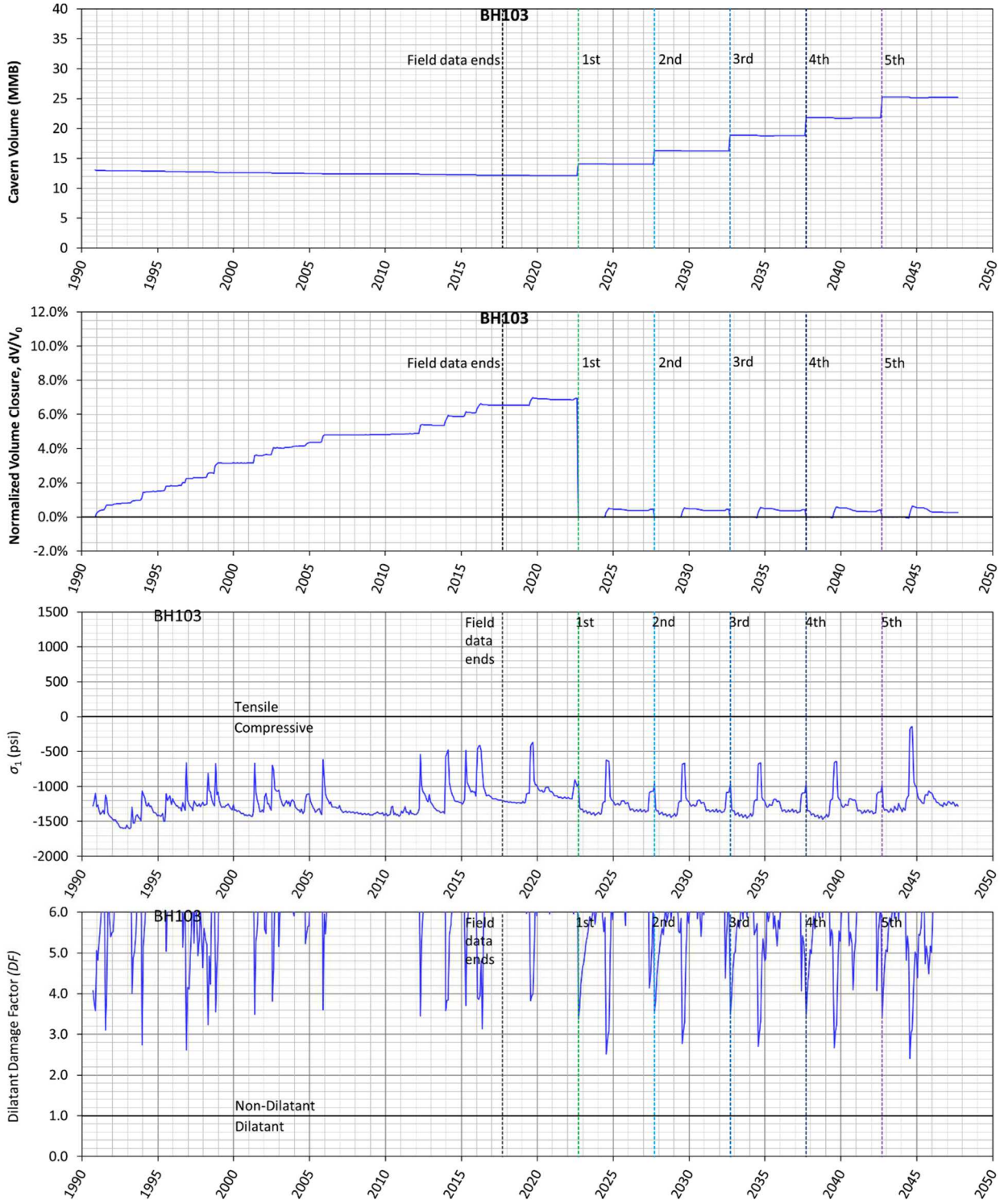

Figure 14. Predicted volumetric change (top), volumetric closure normalized to initial cavern volume of BH-103 (2nd), maximum σ_1 (3rd) and minimum dilatant damage factor (bottom) in the salt surrounding BH-103 over time

5.4. BH-104

Modeling of the leaching process of the caverns is performed by deleting a pre-meshed block of elements along the walls of the cavern so that the cavern volume is increased by 16 percent per drawdown. Figure 15 shows the cavity of BH-104 as developed from sonar data, along with drawdown skins and extra skins. In this simulation, BH-104 is modeled as having five drawdown layers to be removed to account for the future oil drawdown activities.

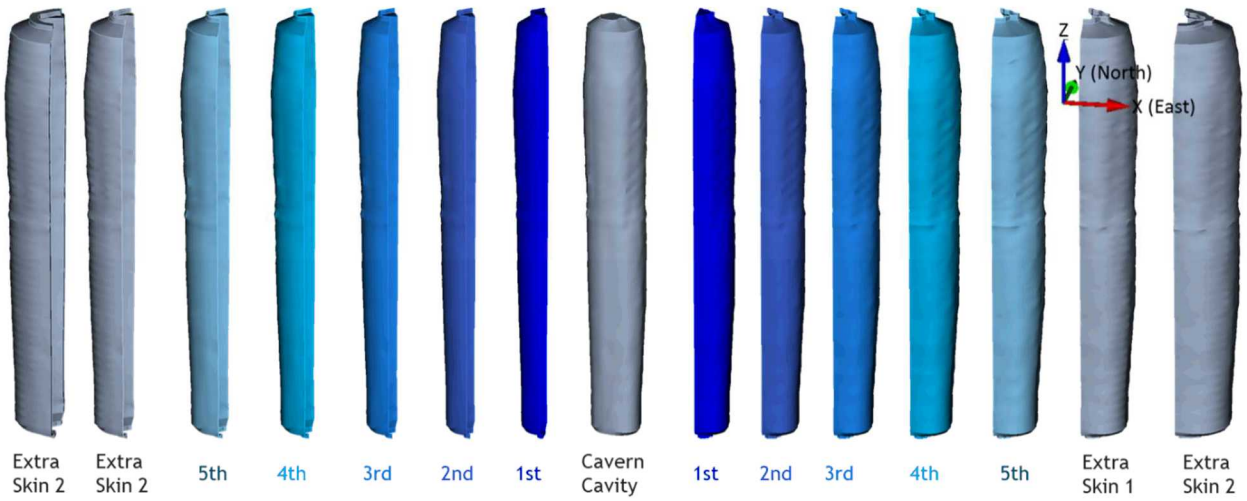

Figure 15. BH-102 cavern cavity with five drawdown skins (leaching layers) and extra skins

Figure 16 shows the predicted volumetric change (top), and volumetric closure normalized to initial cavern volume (2nd panel), maximum σ_1 (3rd panel), and minimum *DF* (bottom) in the salt volume surrounding BH-104 over time. The initial cavern cavity volume was 13.0 MMB on 10/20/1990 and is predicted to be 12.1 MMB on 8/20/2022. The cavern volume is predicted to decrease by 6.8% over 32 years (10/20/1990 - 8/20/2022).

The maximum σ_1 never reaches a positive (tensile stress state) value through five drawdowns, and the minimum *DF* either never reaches to be less than 1 during every workover until the end of simulation. The largest predicted value of the maximum σ_1 is -205 psi on 12/20/2044 during the workover started on 10/1/2044 for 3 months. The smallest predicted value of the minimum *DF* is 2.3 on 1/21/1992 during the workover started on 1/5/1992 for 85 days.

In conclusion, BH-104 is predicted to be structurally stable through the fifth drawdown leach.

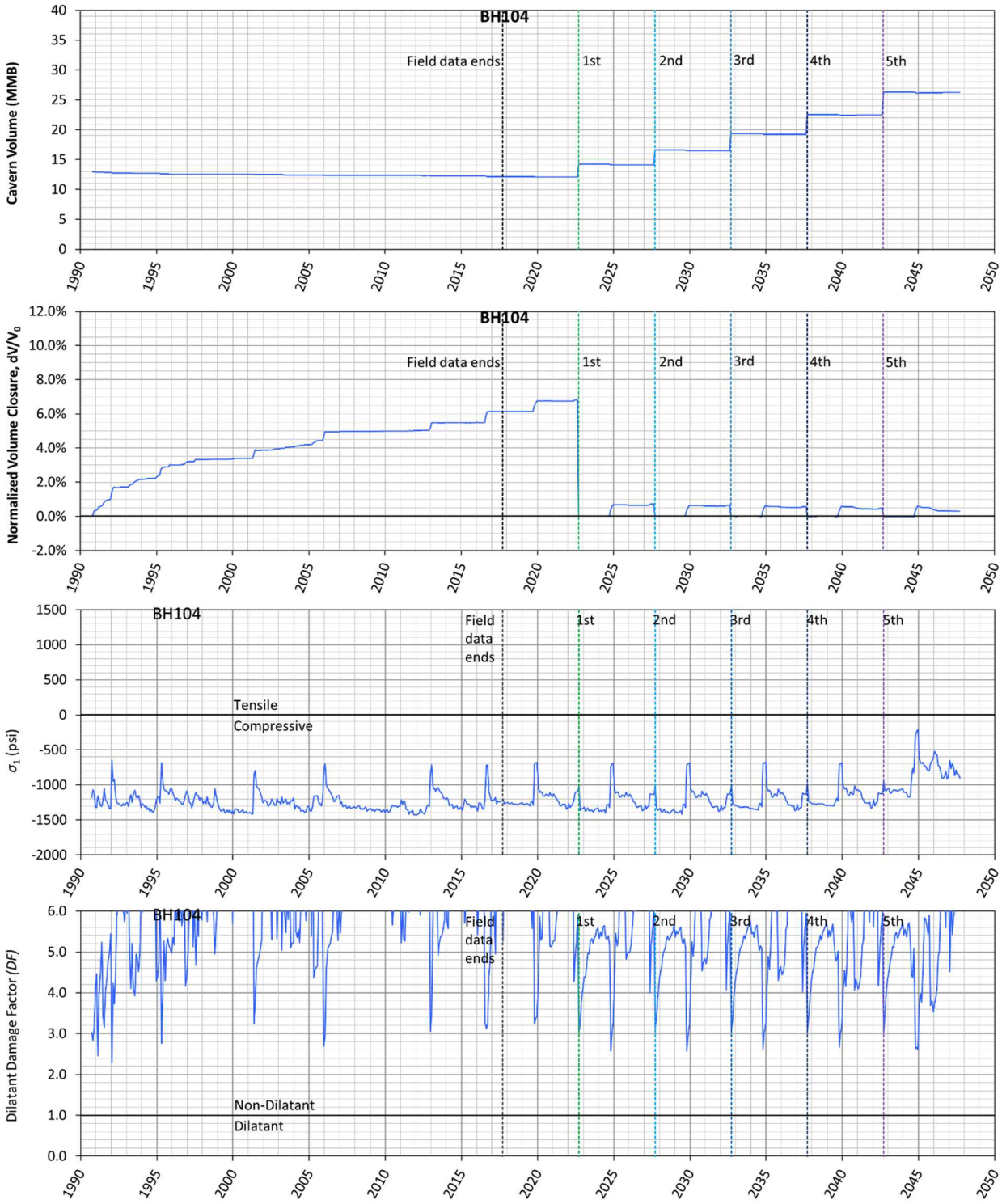

Figure 16. Predicted volumetric change (top), volumetric closure normalized to initial cavern volume of BH-104 (2nd), maximum σ_1 (3rd) and minimum dilatant damage factor (bottom) in the salt surrounding BH-104 over time

5.5. BH-105

Modeling of the leaching process of the caverns is performed by deleting a pre-meshed block of elements along the walls of the cavern so that the cavern volume is increased by 16 percent per drawdown. Figure 17 shows the cavity of BH-105 as developed from sonar data, along with drawdown skins and extra skins. In this simulation, BH-105 is modeled as having five drawdown layers to be removed to account for the future oil drawdown activities.

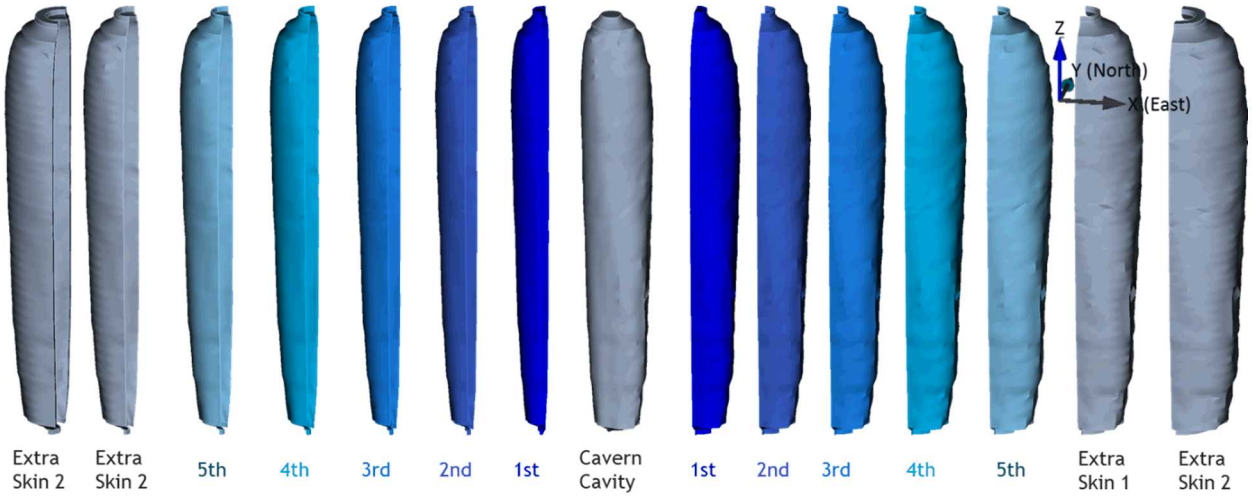

Figure 17. BH-105 cavern cavity with five drawdown skins (leaching layers) and extra skins

Figure 18 shows the predicted volumetric change (top), and volumetric closure normalized to initial cavern volume (2nd panel), maximum σ_1 (3rd panel), and minimum *DF* (bottom) in the salt volume surrounding BH-105 over time. The initial cavern cavity volume was 13.0 MMB on 5/21/1990 and is predicted to be 11.9 MMB on 8/20/2022. The cavern volume is predicted to decrease by 8.2% over 32 years (5/21/1990 - 8/20/2022).

The maximum σ_1 reaches a positive (tensile stress state) value during the workovers started on 5/14/2010 for 412 days. The maximum σ_1 are calculated to be 233 psi on 6/22/2011 (2011.47 year). The value of maximum σ_1 goes up and down with zero until 9/18/2017. The second peak appears on 9/20/2022 (2022.72 year) and calculated to be 21 psi. The positive peaks appear during the workovers after the 3rd drawdown leach. The maximum σ_1 are calculated to be 397, 920, and 1550 psi at 2035.22, 2040.22, and 2045.22 years, respectively. Figure 19 shows the contour plots of σ_1 on the specific times to show the area in tension in the cavern skin layers during the workovers at 2011.47, 2020.22, 2040.22, and 2045.22 years. The areas in tensile state are located at the floor edge. The tensile state may occur not at vertical wall but floor because of the geometry of the edge and floor.

The minimum *DF* reaches less than 1 (onset of dilatant damage) during the workovers started on 1/1/2035 for three months when the maximum σ_1 reaches a positive (tensile stress state) value simultaneously. The minimum *DF* is calculated to be 0.98 on 3/23/2035 (2035.22 year). The peak values of *DF* appear during every workover as shown in Figure 18. The minimum *DF* are calculated to be 0.0017, 0.13, and 0.4 at 2040.30, 2042.55, and 2045.22 years, respectively. Figure 20 shows the

contour plots of *DF* at specific times to show the areas in dilatant damage state (*DF*<1) in the cavern skin layers after each drawdown leach. The areas in dilatant damaged are located at the floor edge. The dilatant state may occur because of the geometry of the edge of floor, but not vertical wall. The consequences of a salt fracture here are minimal, because the predicted dilatant and tensile stresses are confined to a small area at the bottom of the cavern, and it is unlikely to propagate to a nearby cavern. Additionally, it is in the brine-filled portion of the cavern, so oil loss to the formation is highly unlikely. This implies it does not affect the cavern structural stability.

In conclusion, BH-105 is expected to be structurally stable until the fifth drawdown leach. However, the dilatant damaged areas in tensile stress state are created on the floor edge of the cavern during the workovers. Therefore, we recommend a re-examination of the cavern stability with a new cavern volume obtained from a sonar after a drawdown leach is completed in the future.

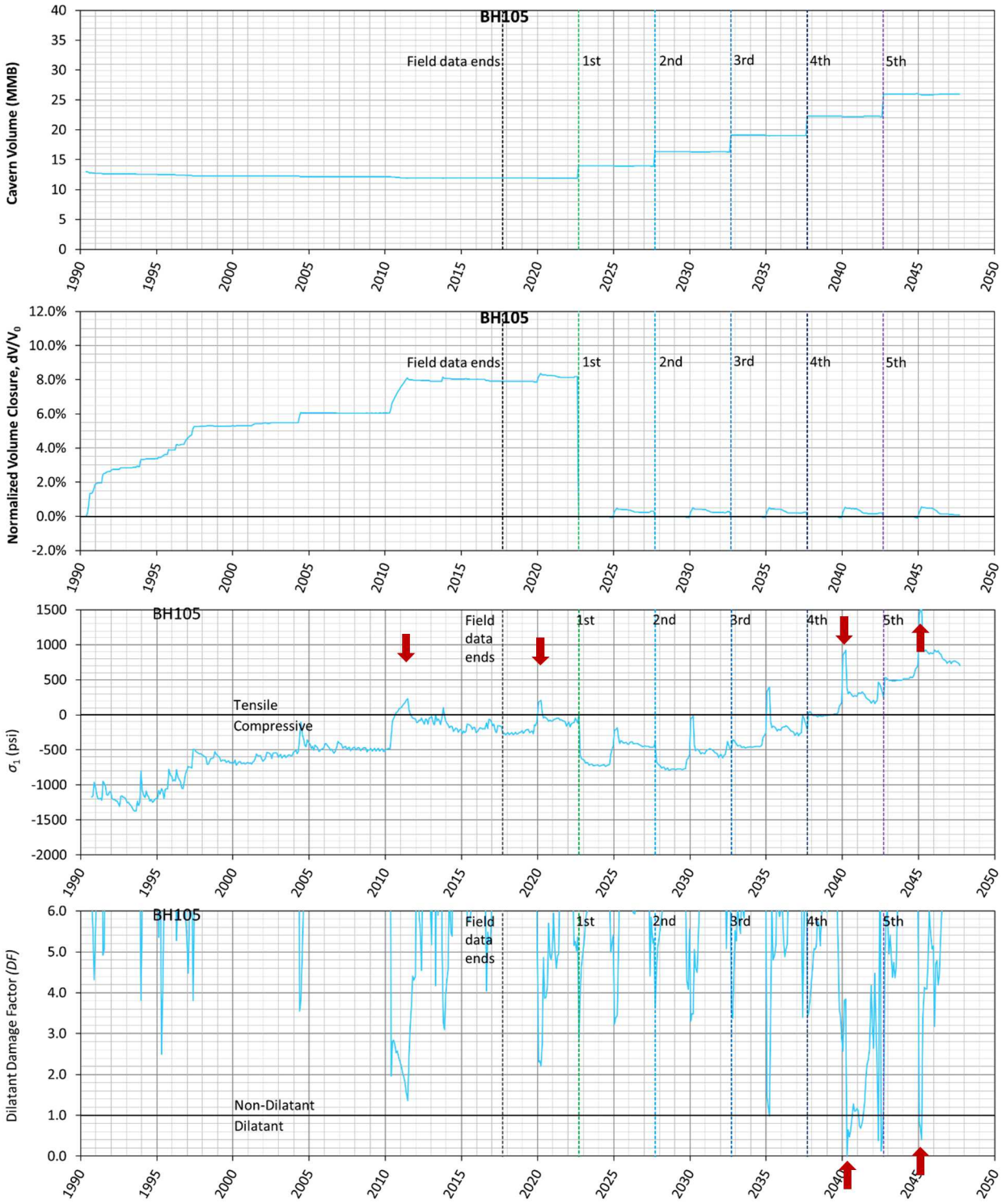

Figure 18. Predicted volumetric change (top), volumetric closure normalized to initial cavern volume of BH-105 (2nd), maximum σ_1 (3rd) and minimum dilatant damage factor (bottom) in the salt surrounding BH-105 over time

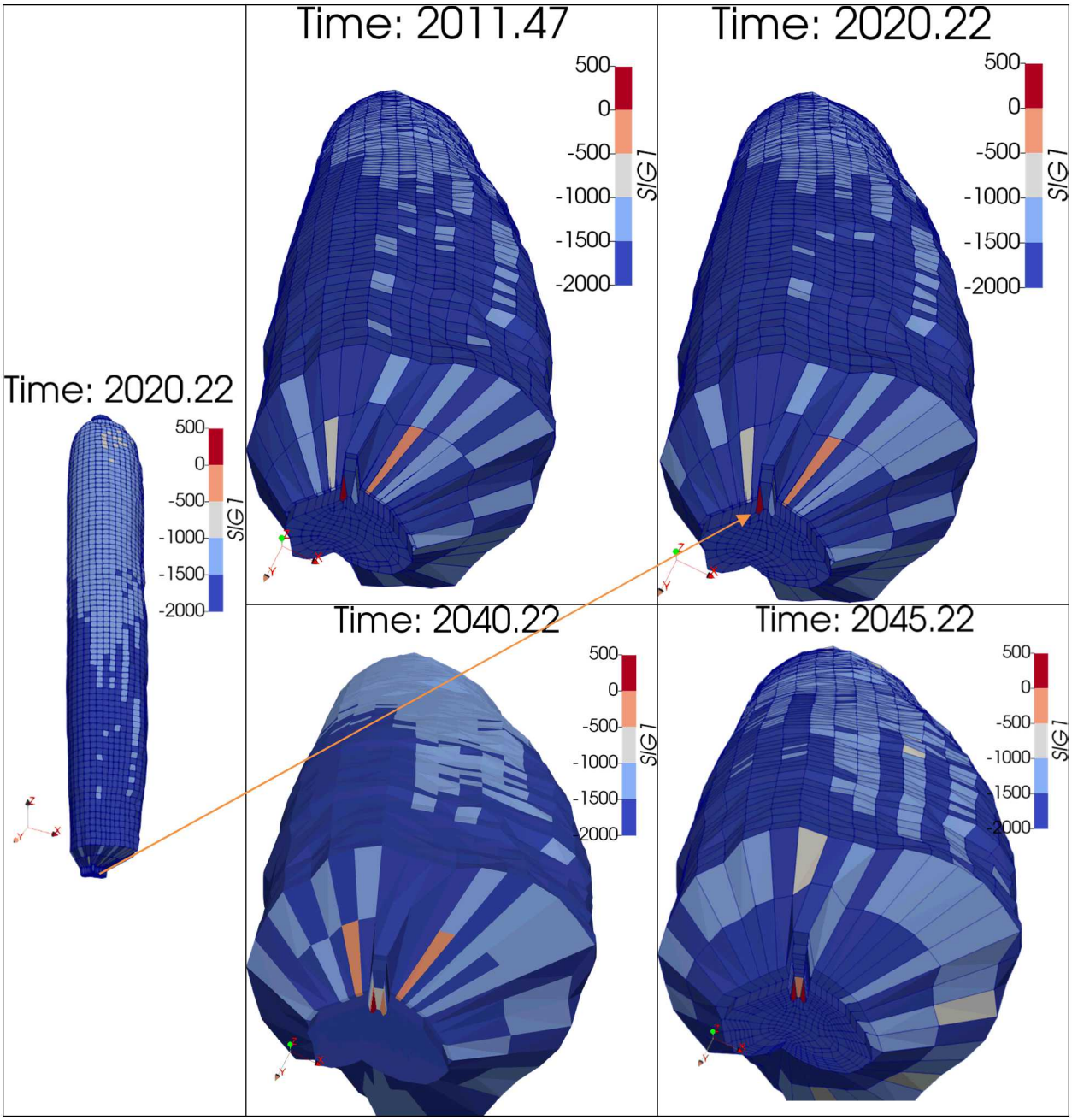

Figure 19. Contour plots of σ_1 on specific dates. Areas in tensile state are shown in red ($\sigma_1 > 0$). Each value of maximum σ_1 are indicated by each arrow at each specific time on the 3rd panel in Figure 18

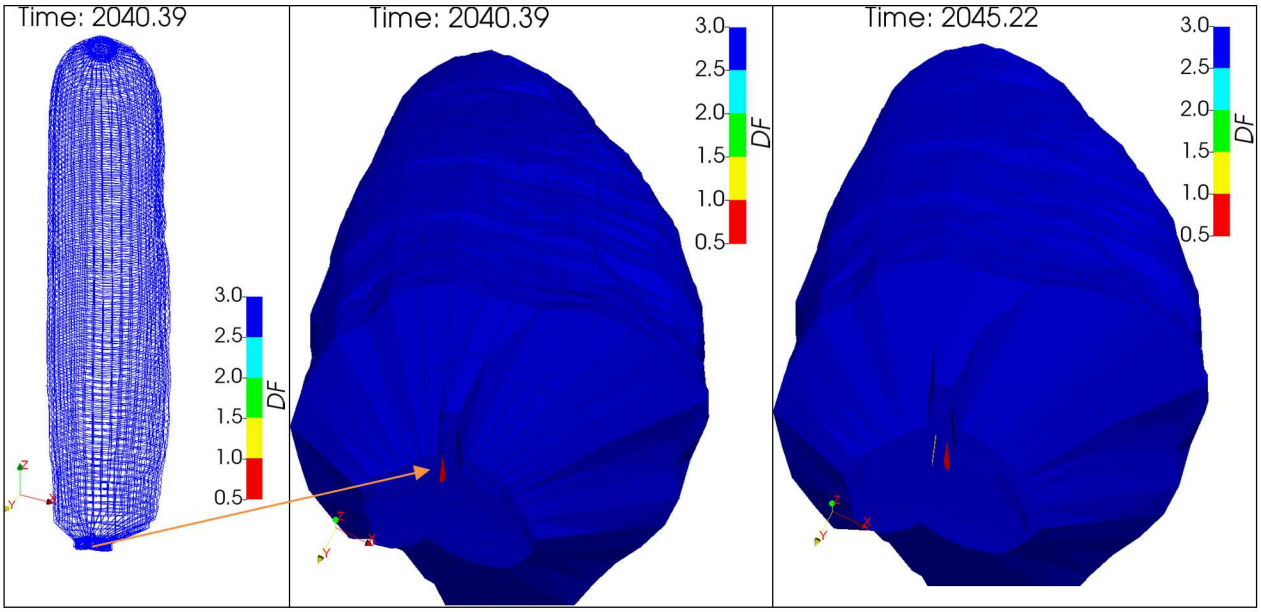

Figure 20. Contour plots of *DF* on specific dates. Areas in dilatant are shown in red (*DF* < 1). Each value of minimum *DF* is indicated by each arrow at each specific time on the bottom panel in Figure 18

5.6. BH-106

Modeling of the leaching process of the caverns is performed by deleting a pre-meshed block of elements along the walls of the cavern so that the cavern volume is increased by 16 percent per drawdown. Figure 21 shows the cavity of BH-106 as developed from sonar data, along with drawdown skins and extra skins. In this simulation, BH-106 is modeled as having five drawdown layers to be removed to account for the future oil drawdown activities.

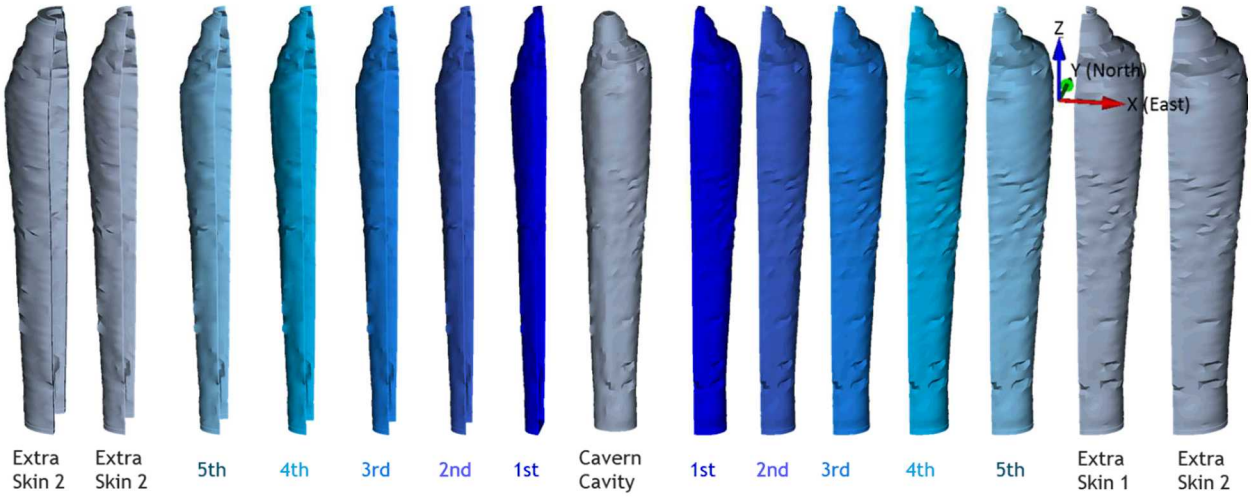

Figure 21. BH-106 cavern cavity with five drawdown skins (leaching layers) and extra skins

Figure 22 shows the predicted volumetric change (top), and volumetric closure normalized to initial cavern volume (2nd panel), maximum σ_1 (3rd panel), and minimum *DF* (bottom) in the salt volume surrounding BH-106 over time. The initial cavern cavity volume was 13.1 MMB on 10/20/1990 and is predicted to be 12.5 MMB on 8/20/2022. The cavern volume is predicted to decrease by 4.7% over 32 years (12/20/1990 - 8/20/2022).

The maximum σ_1 never reaches a positive (tensile stress state) value through five drawdowns, and the minimum *DF* either never reaches to be less than 1 during every workover until the end of simulation. The largest predicted value of the maximum σ_1 is -427 psi on 6/20/2097 during the workover started on 1/17/1997 for 229 days. The smallest predicted value of the minimum *DF* is 2.06 on 4/22/1991 during the workover started on 4/15/1991 for 20 days.

In conclusion, BH-106 is predicted to be structurally stable through the fifth drawdown leach.

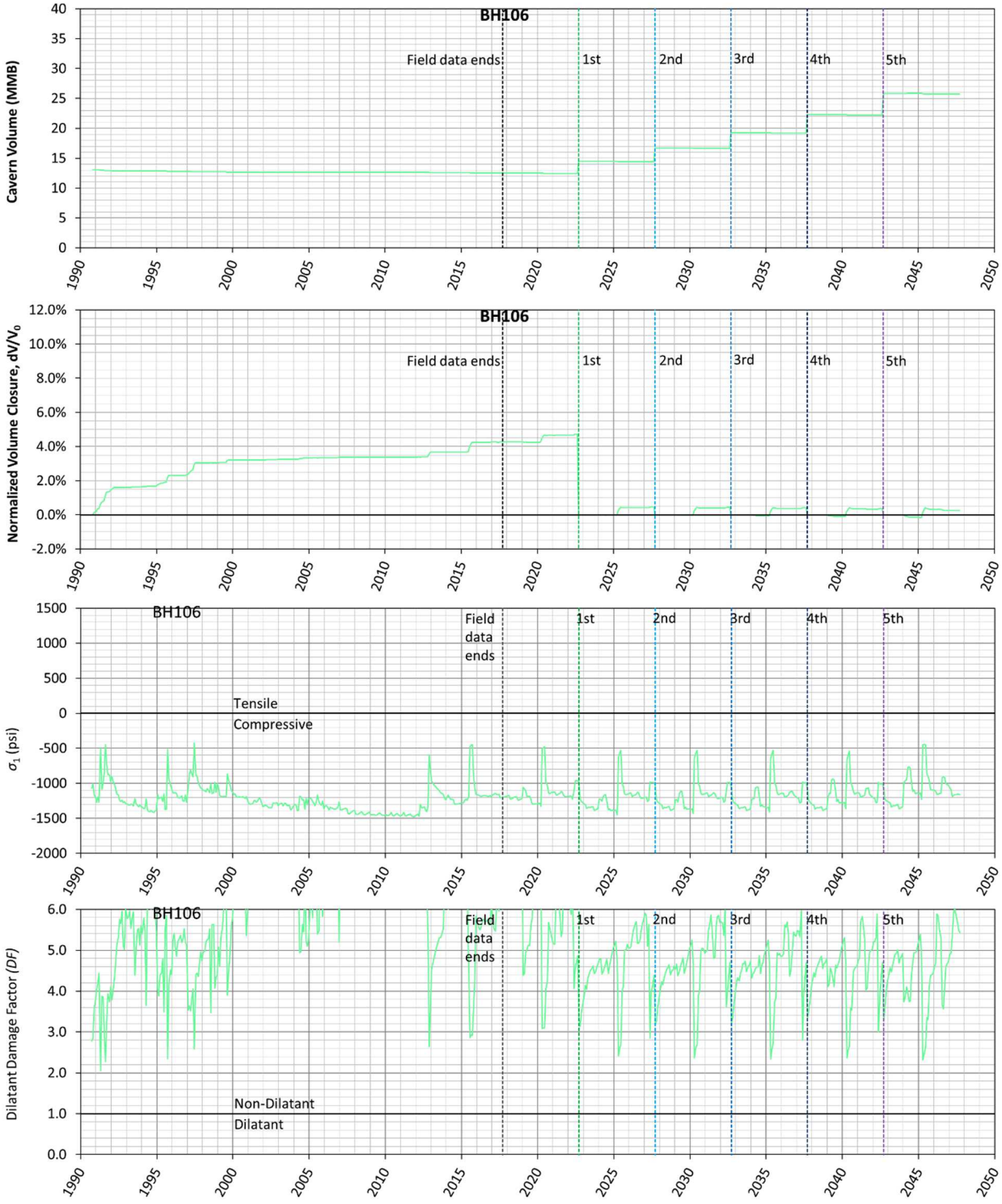

Figure 22. Predicted volumetric change (top), volumetric closure normalized to initial cavern volume of BH-106 (2nd), maximum σ_1 (3rd) and minimum dilatant damage factor (bottom) in the salt surrounding BH-106 over time

5.7. BH-107

Modeling of the leaching process of the caverns is performed by deleting a pre-meshed block of elements along the walls of the cavern so that the cavern volume is increased by 16 percent per drawdown. Figure 23 shows the cavity of BH-107 as developed from sonar data, along with drawdown skins and extra skins. In this simulation, BH-107 is modeled as having five drawdown layers to be removed to account for the future oil drawdown activities.

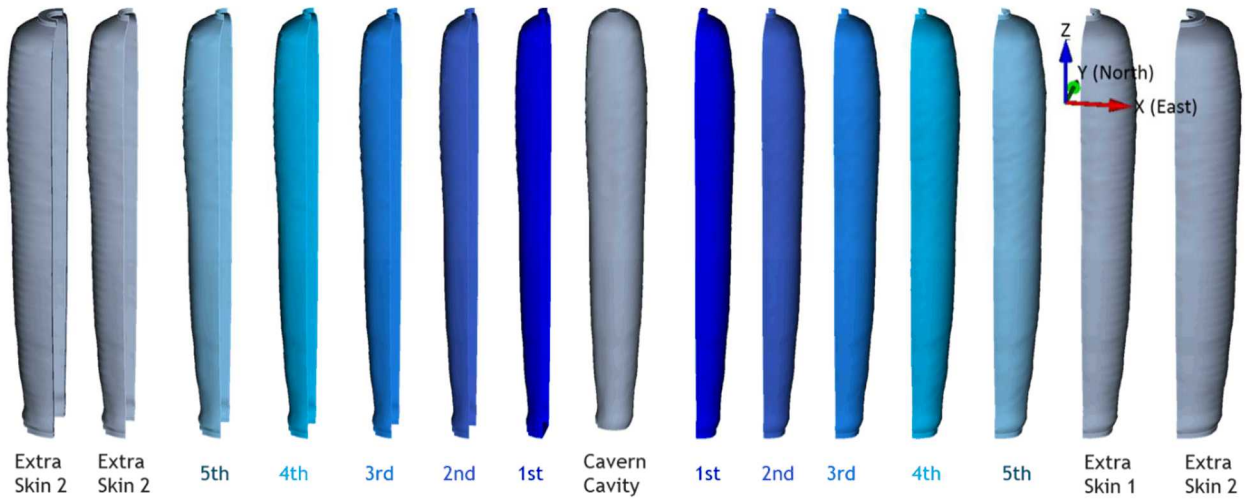

Figure 23. BH-107 cavern cavity with five drawdown skins (leaching layers) and extra skins

Figure 24 shows the predicted volumetric change (top), and volumetric closure normalized to initial cavern volume (2nd panel), maximum σ_1 (3rd panel), and minimum *DF* (bottom) in the salt volume surrounding BH-107 over time. The initial cavern cavity volume was 12.8 MMB on 4/20/1990 and is predicted to be 12.0 MMB on 8/20/2022. The cavern volume is predicted to decrease by 6.1% over 32 years (4/20/1990 - 8/20/2022).

The maximum σ_1 never reaches a positive (tensile stress state) value through five drawdowns, and the minimum *DF* either never reaches to be less than 1 during every workover until the end of simulation. The largest predicted value of the maximum $\sigma_1$is -708 psi on 8/21/1991 during the workover started on 7/22/1991 for 60 days. The smallest predicted value of the minimum *DF* is 2.65 on 6/20/1997 during the workover started on 3/28/1997 for 126 days.

In conclusion, BH-107 is predicted to be structurally stable through the fifth drawdown leach.

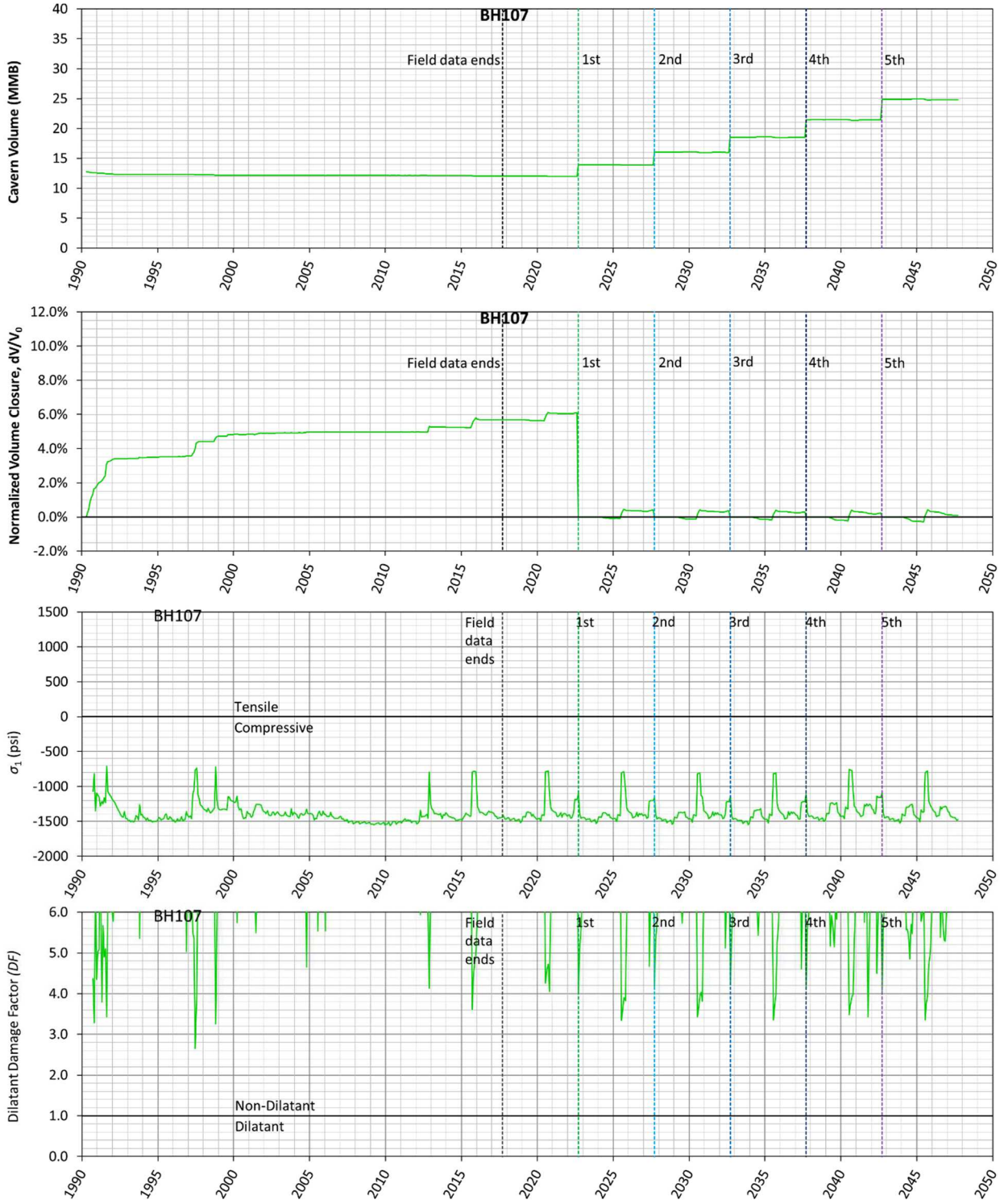

Figure 24. Predicted volumetric change (top), volumetric closure normalized to initial cavern volume of BH-107 (2nd), maximum σ_1 (3rd) and minimum dilatant damage factor (bottom) in the salt surrounding BH-107 over time

5.8. BH-108

Modeling of the leaching process of the caverns is performed by deleting a pre-meshed block of elements along the walls of the cavern so that the cavern volume is increased by 16 percent per drawdown. Figure 25 shows the cavity of BH-108 as developed from sonar data, along with drawdown skins and extra skins. In this simulation, BH-108 is modeled as having five drawdown layers to be removed to account for the future oil drawdown activities.

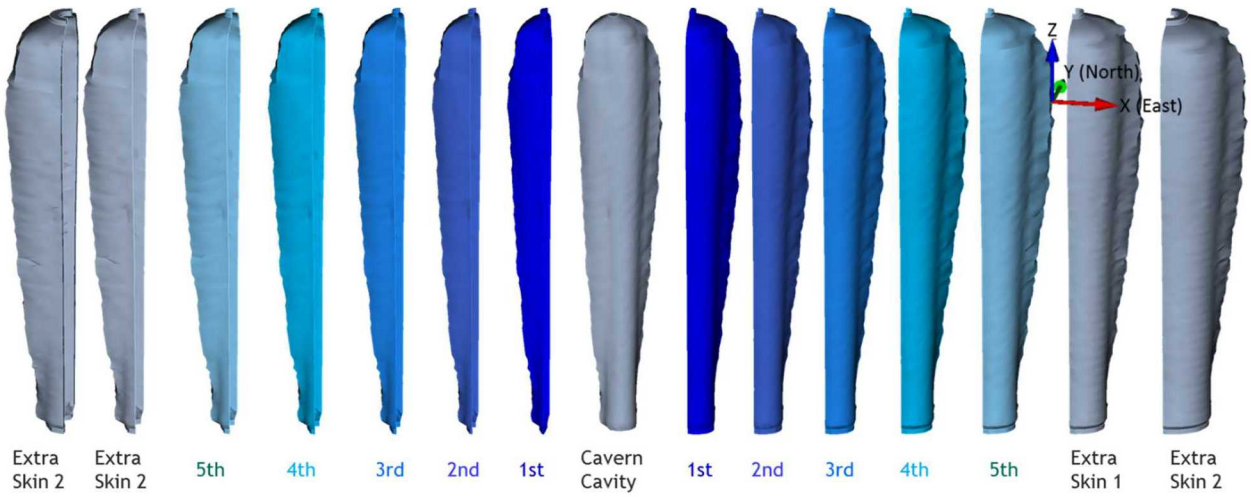

Figure 25. BH-108 cavern cavity with five drawdown skins (leaching layers) and extra skins

Figure 26 shows the predicted volumetric change (top), and volumetric closure normalized to initial cavern volume (2nd panel), maximum σ_1 (3rd panel), and minimum *DF* (bottom) in the salt volume surrounding BH-108 over time. The initial cavern cavity volume was 11.7 MMB on 6/20/1990 and is predicted to be 11.0 MMB on 8/20/2022. The cavern volume is predicted to decrease by 5.6% over 32 years (6/20/1990 - 8/20/2022).

The maximum σ_1 never reaches a positive (tensile stress state) value through five drawdowns, and the minimum *DF* either never reaches to be less than 1 during every workover until the end of simulation. The largest predicted value of the maximum σ_1 is -312 psi on 12/20/2020 during the workover started on 10/1/2020 for three months. The smallest predicted value of the minimum *DF* is 3.09 on 12/21/2003 during the workover started on 10/16/2003 for 89 days.

In conclusion, BH-108 is predicted to be structurally stable through the fifth drawdown leach.

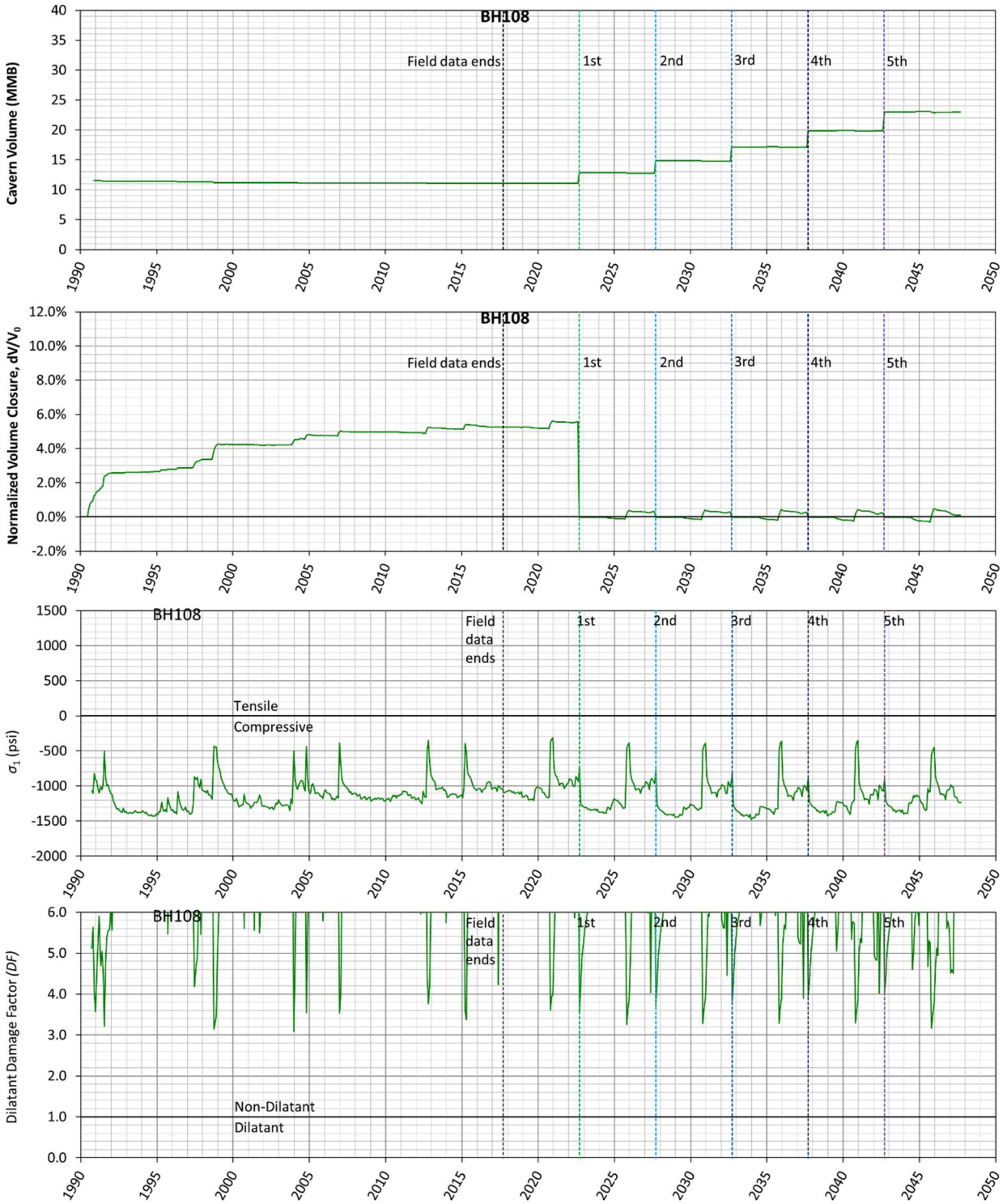

Figure 26. Predicted volumetric change (top), volumetric closure normalized to initial cavern volume of BH-108 (2nd), maximum σ_1 (3rd) and minimum dilatant damage factor (bottom) in the salt surrounding BH-108 over time

5.9. BH-109

Modeling of the leaching process of the caverns is performed by deleting a pre-meshed block of elements along the walls of the cavern so that the cavern volume is increased by 16 percent per drawdown. Figure 27 shows the cavity of BH-109 as developed from sonar data, along with drawdown skins and extra skins. In this simulation, BH-109 is modeled as having five drawdown layers to be removed to account for the future oil drawdown activities.

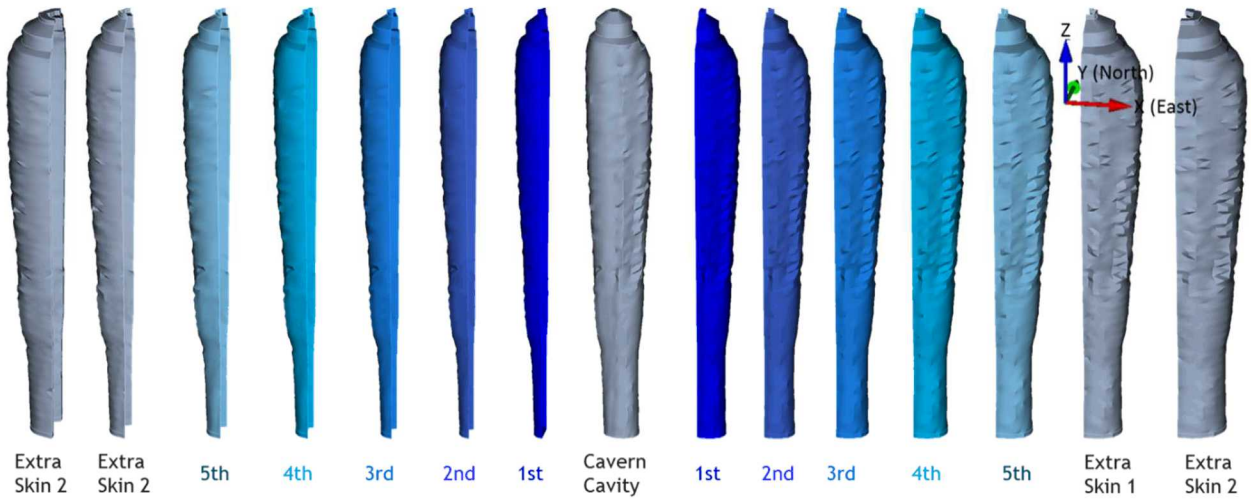

Figure 27. BH-109 cavern cavity with five drawdown skins (leaching layers) and extra skins

Figure 28 shows the predicted volumetric change (top), and volumetric closure normalized to initial cavern volume (2nd panel), maximum σ_1 (3rd panel), and minimum *DF* (bottom) in the salt volume surrounding BH-109 over time. The initial cavern cavity volume was 12.9 MMB on 7/21/1990 and is predicted to be 12.2 MMB on 8/20/2022. The cavern volume is predicted to decrease by 6.0% over 32 years (7/21/1990 - 8/20/2022).

The maximum σ_1 never reaches a positive (tensile stress state) value through five drawdowns, and the minimum *DF* either never reaches to be less than 1 during every workover until the end of simulation. The largest predicted value of the maximum σ_1 is -470 psi on 3/22/2046 during the workover started on 1/1/2046 for three months. The smallest predicted value of the minimum *DF* is 2.73 on 1/21/2036 during the workover started on 1/1/2036 for three months.

In conclusion, BH-109 is predicted to be structurally stable through the fifth drawdown leach.

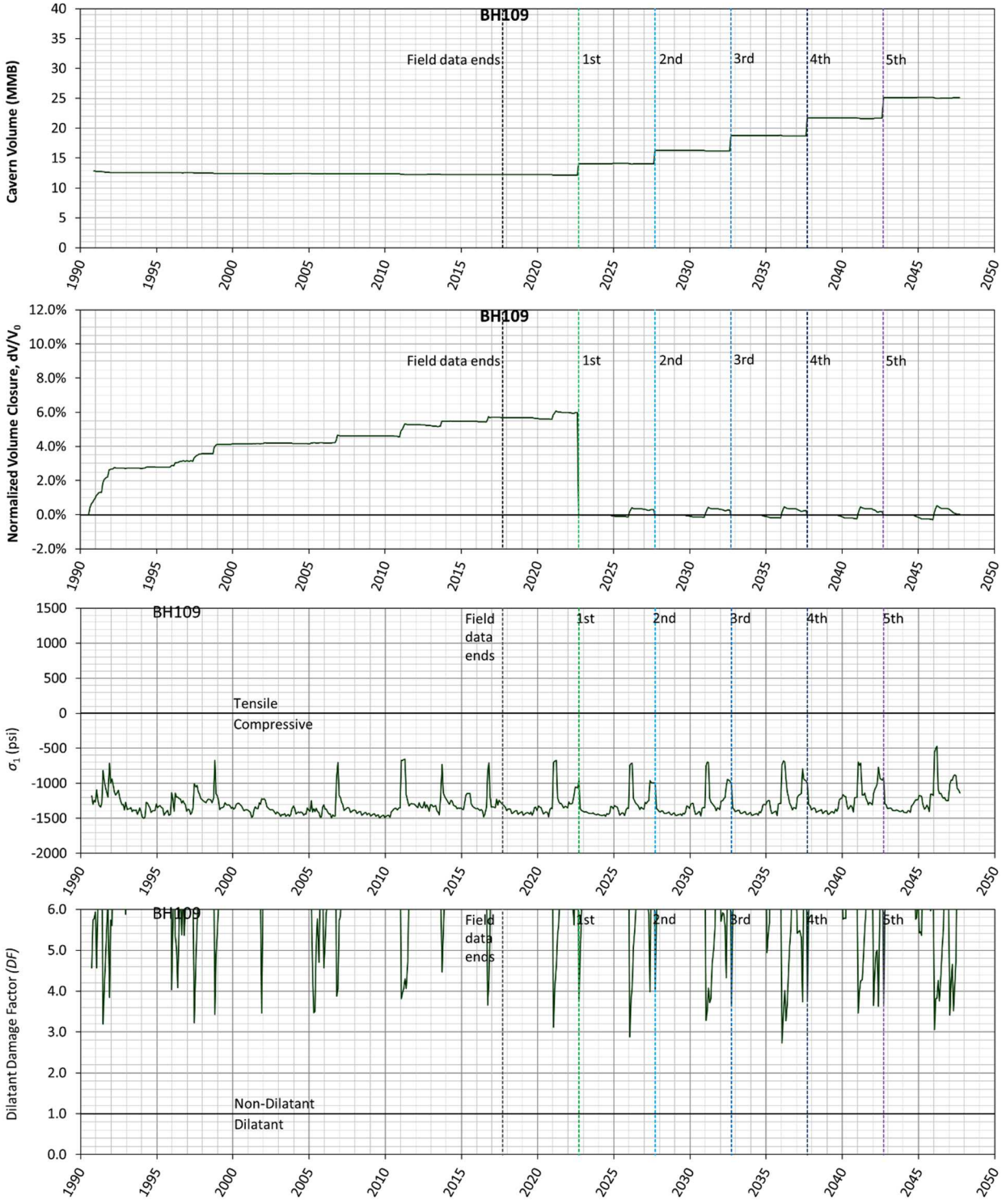

Figure 28. Predicted volumetric change (top), volumetric closure normalized to initial cavern volume of BH-109 (2nd), maximum σ_1 (3rd) and minimum dilatant damage factor (bottom) in the salt surrounding BH-109 over time

5.10. BH-110

Modeling of the leaching process of the caverns is performed by deleting a pre-meshed block of elements along the walls of the cavern so that the cavern volume is increased by 16 percent per drawdown. Figure 29 shows the cavity of BH-110 as developed from sonar data, along with drawdown skins and extra skins. In this simulation, BH-110 is modeled as having five drawdown layers to be removed to account for the future oil drawdown activities.

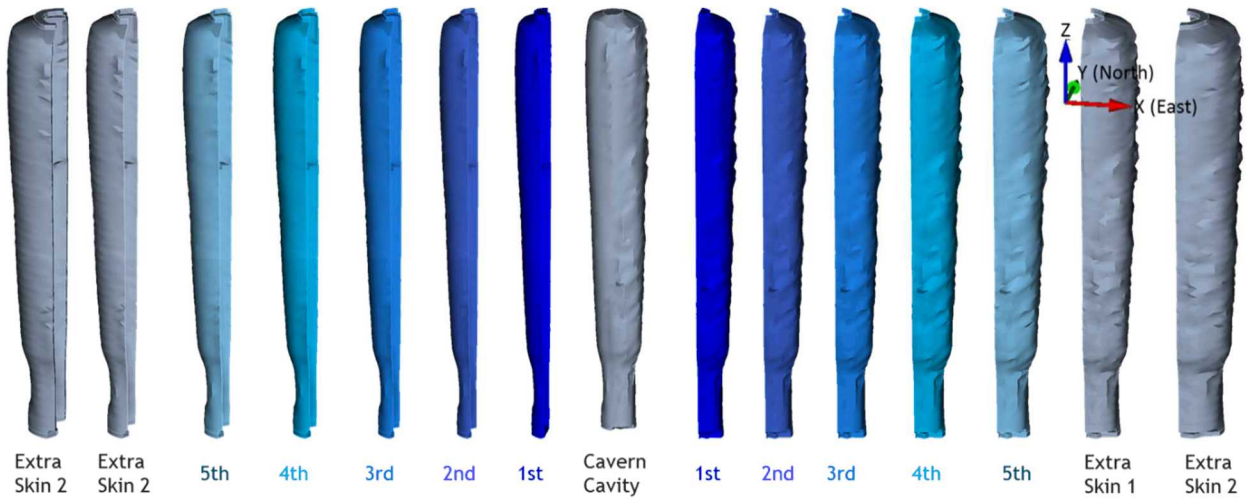

Figure 29. BH-110 cavern cavity with five drawdown skins (leaching layers) and extra skins

Figure 30 shows the predicted volumetric change (top), and volumetric closure normalized to initial cavern volume (2nd panel), maximum σ_1 (3rd panel), and minimum *DF* (bottom) in the salt volume surrounding BH-110 over time. The initial cavern cavity volume was 13.0 MMB on 4/20/1990 and is predicted to be 12.1 MMB on 8/20/2022. The cavern volume is predicted to decrease by 6.9% over 32 years (4/20/1990 - 8/20/2022).

The maximum σ_1 never reaches a positive (tensile stress state) value through five drawdowns, and the minimum *DF* either never reaches to be less than 1 during every workover until the end of simulation. The largest predicted value of the maximum σ_1 is -129 psi on 6/20/2026 during the workover started on 4/1/2026 for three months. The smallest predicted value of the minimum *DF* is 2.30 on 4/20/2026 during the workover started on 4/1/2026 for three months.

In conclusion, BH-110 is predicted to be structurally stable through the fifth drawdown leach.

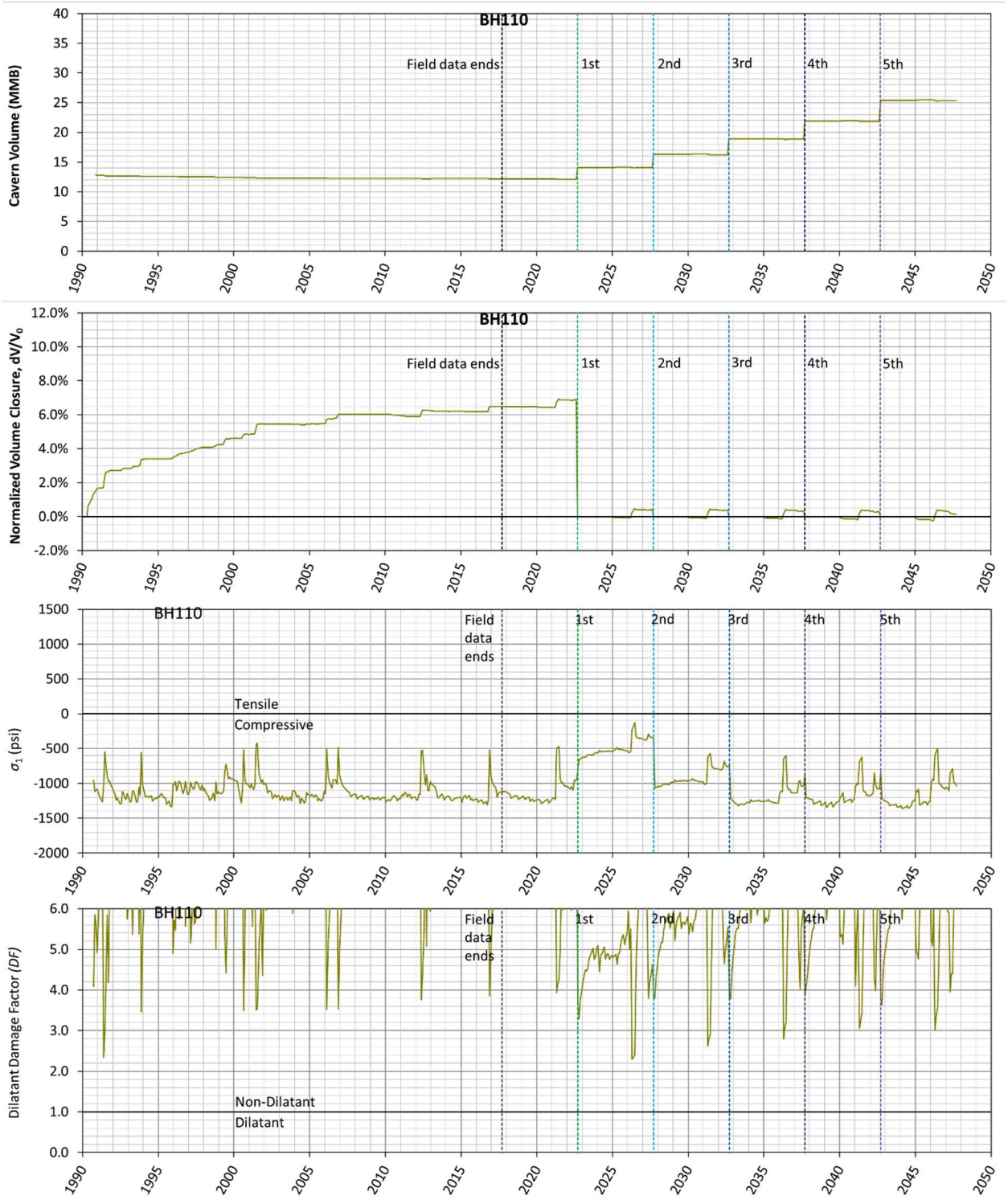

Figure 30. Predicted volumetric change (top), volumetric closure normalized to initial cavern volume of BH-110 (2nd), maximum σ_1 (3rd) and minimum dilatant damage factor (bottom) in the salt surrounding BH-110 over time

5.11. BH-111

Modeling of the leaching process of the caverns is performed by deleting a pre-meshed block of elements along the walls of the cavern so that the cavern volume is increased by 16 percent per drawdown. Figure 31 shows the cavity of BH-111 as developed from sonar data, along with drawdown skins and extra skins. In this simulation, BH-111 is modeled as having five drawdown layers to be removed to account for the future oil drawdown activities.

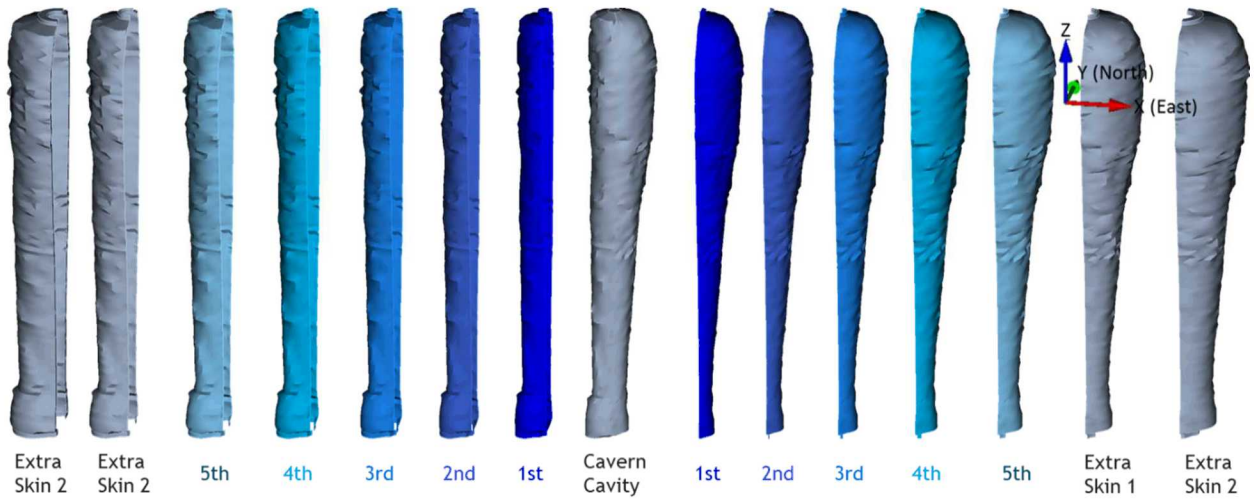

Figure 31. BH-111 cavern cavity with five drawdown skins (leaching layers) and extra skins

Figure 32 shows the predicted volumetric change (top), and volumetric closure normalized to initial cavern volume (2nd panel), maximum σ_1 (3rd panel), and minimum *DF* (bottom) in the salt volume surrounding BH-111 over time. The initial cavern cavity volume was 13.3 MMB on 7/21/1991 and is predicted to be 13.1 MMB on 8/20/2022. The cavern volume is predicted to decrease by 2.9% over 31 years (7/21/1991 - 8/20/2022). The amount of volume closure is smaller than that of other SPR caverns because the lower volume of cavity is relatively small. The creep closure rate increases with depth because the difference between lithostatic and cavern internal pressures increases.

The maximum σ_1 never reaches a positive (tensile stress state) value through five drawdowns, and the minimum *DF* either never reaches to be less than 1 during every workover until the end of simulation. The largest predicted value of the maximum σ_1 is -290 psi on 3/22/2017 during the workover started on 11/23/2016 for 129 days. The smallest predicted value of the minimum *DF* is 1.36 on 7/22/2036 during the workover started on 7/1/2036 for three months.

In conclusion, BH-111 is predicted to be structurally stable through the fifth drawdown leach.

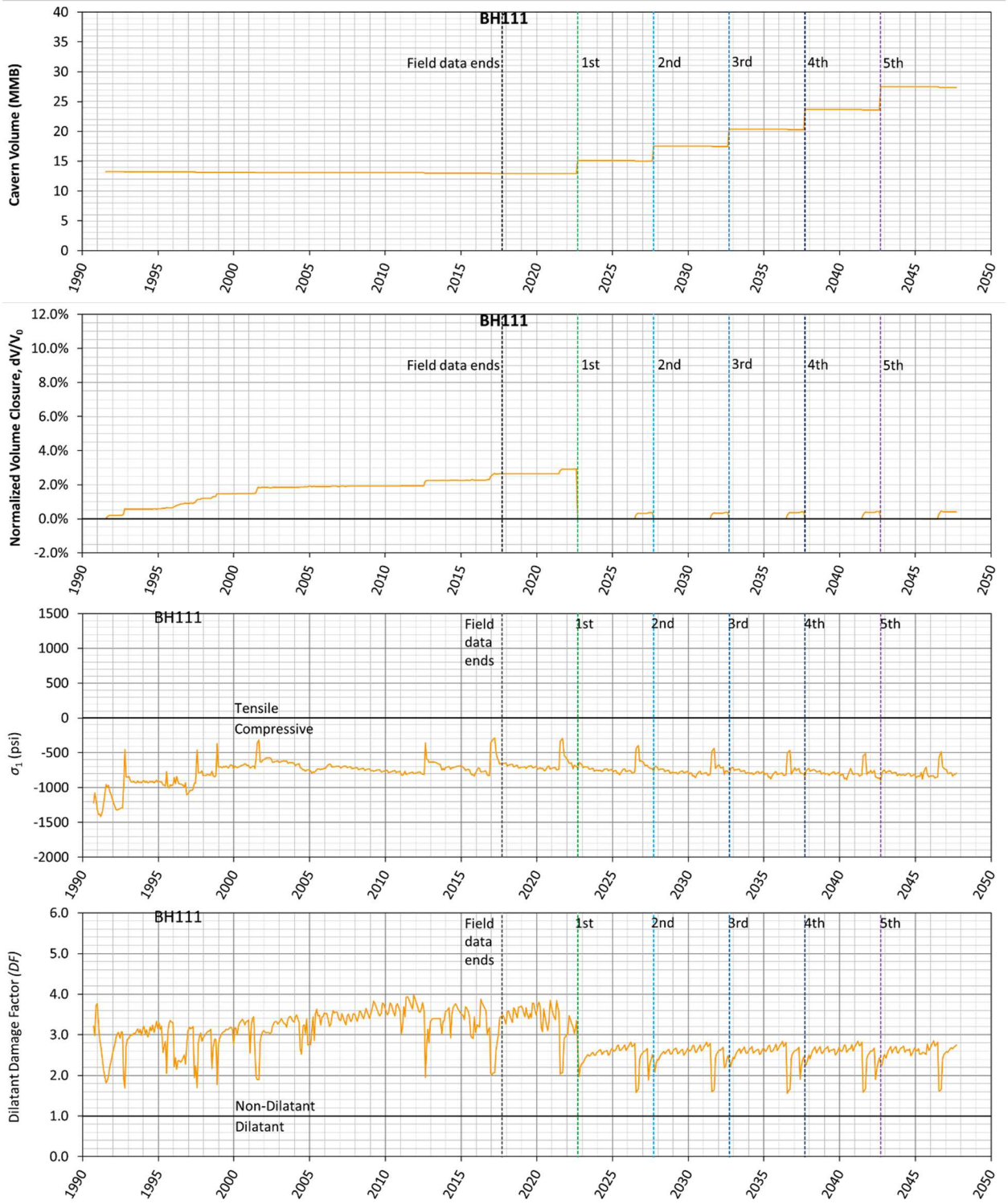

Figure 32. Predicted volumetric change (top), volumetric closure normalized to initial cavern volume of BH-111 (2nd), maximum σ_1 (3rd) and minimum dilatant damage factor (bottom) in the salt surrounding BH-111 over time

5.12. BH-112

Modeling of the leaching process of the caverns is performed by deleting a pre-meshed block of elements along the walls of the cavern so that the cavern volume is increased by 16 percent per drawdown. Figure 33 shows the cavity of BH-112 as developed from sonar data, along with drawdown skins and extra skins. In this simulation, BH-112 is modeled as having five drawdown layers to be removed to account for the future oil drawdown activities.

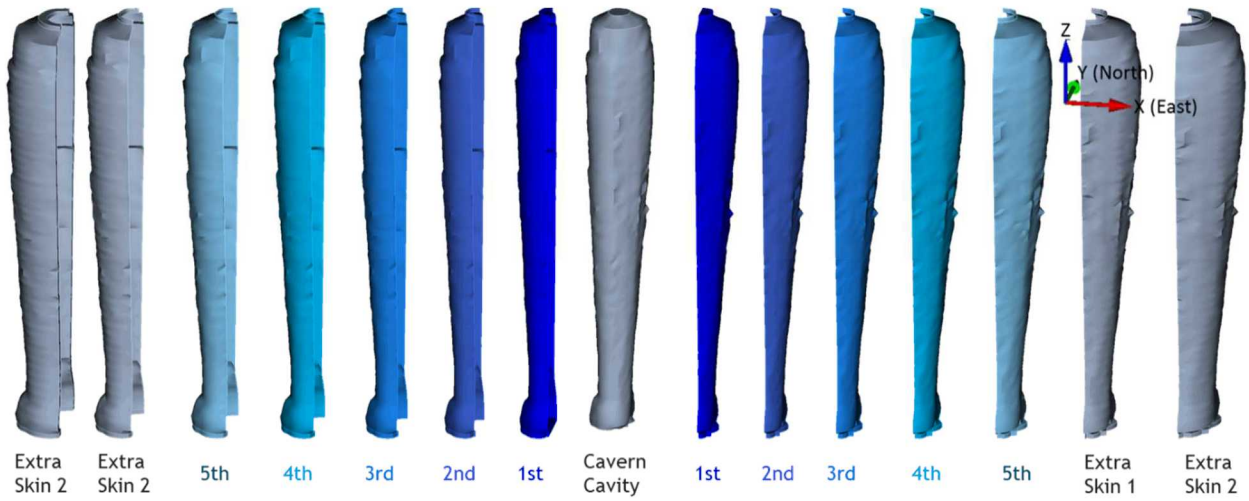

Figure 33. BH-112 cavern cavity with five drawdown skins (leaching layers) and extra skins

Figure 34 shows the predicted volumetric change (top), and volumetric closure normalized to initial cavern volume (2nd panel), maximum σ_1 (3rd panel), and minimum *DF* (bottom) in the salt volume surrounding BH-112 over time. The initial cavern cavity volume was 13.1 MMB on 6/21/1991 and is predicted to be 12.9 MMB on 8/20/2022. The cavern volume is predicted to decrease by 2.0% over 31 years (6/21/1991 - 8/20/2022). The amount of volume closure is relatively small because the lower volume of cavity is small like BH-111.

The maximum σ_1 never reaches a positive (tensile stress state) value through five drawdowns, and the minimum *DF* either never reaches to be less than 1 during every workover until the end of simulation. The largest predicted value of the maximum σ_1 is -266 psi on 9/20/2045 during the workover of BH-107 started on 7/1/2045 for three months. The peaks appear during the workovers of BH-107, BH-108, BH-112 itself, and BH-113 since the 1st drawdown of 14 caverns occurs. BH-107, BH-108, and BH-113 are neighbor caverns as shown in Figure 1. This implies that the volume closure of neighbor caverns affects the behavior of BH-112. The smallest predicted value of the minimum *DF* is 1.17 on 10/21/2026 during the workover started on 10/1/2026 for three months.

In conclusion, BH-112 is predicted to be structurally stable through the fifth drawdown leach.

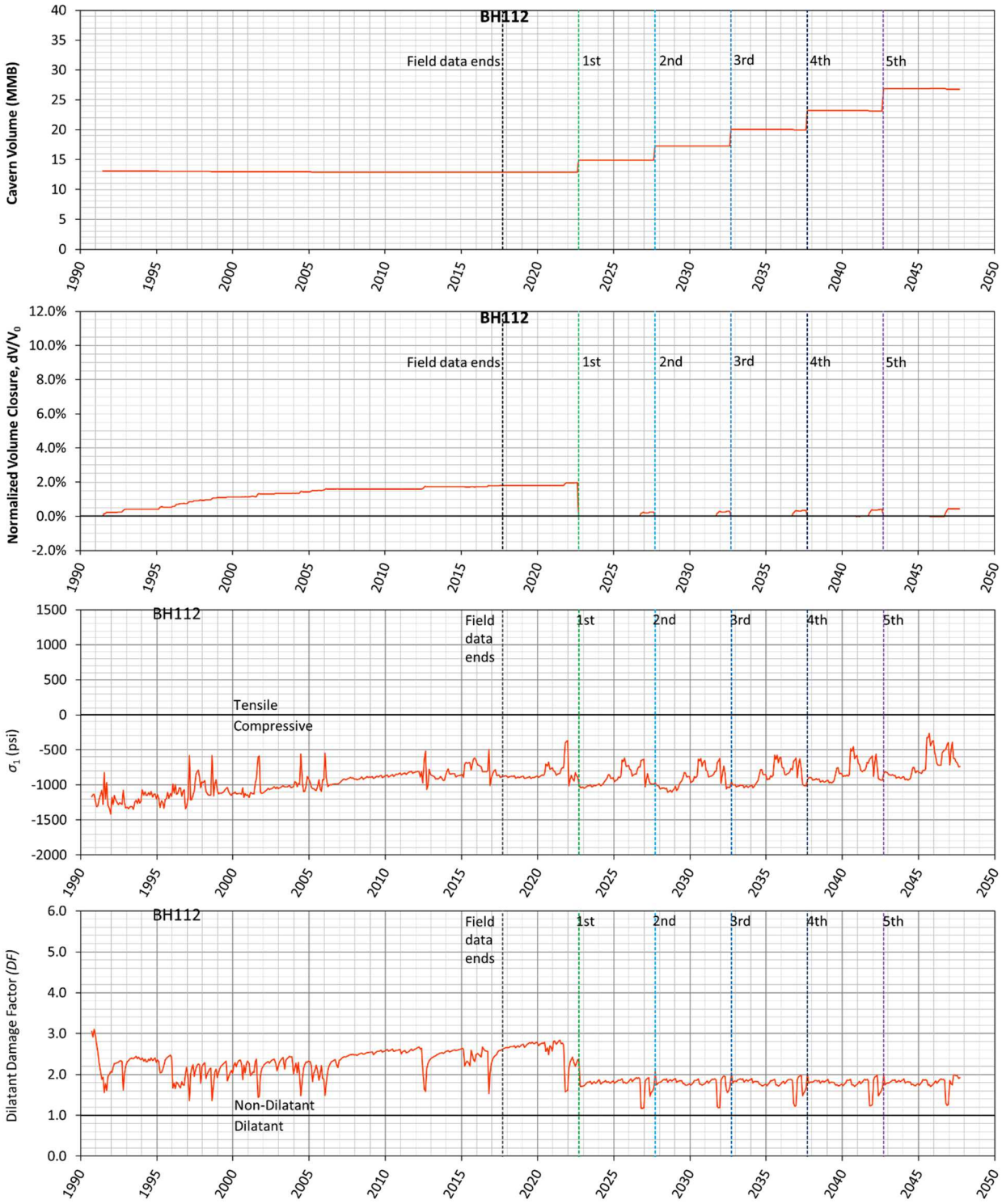

Figure 34. Predicted volumetric change (top), volumetric closure normalized to initial cavern volume of BH-112 (2nd), maximum σ_1 (3rd) and minimum dilatant damage factor (bottom) in the salt surrounding BH-112 over time

5.13. BH-113

Modeling of the leaching process of the caverns is performed by deleting a pre-meshed block of elements along the walls of the cavern so that the cavern volume is increased by 16 percent per drawdown. Figure 35 shows the cavity of BH-113 as developed from sonar data, along with drawdown skins and extra skins. In this simulation, BH-113 is modeled as having five drawdown layers to be removed to account for the future oil drawdown activities.

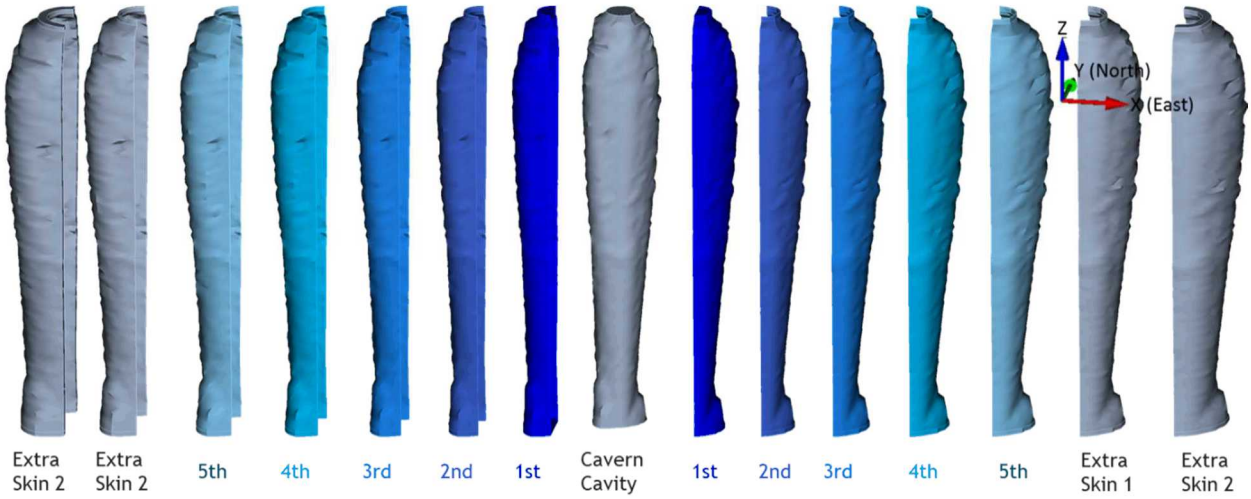

Figure 35. BH-113 cavern cavity with five drawdown skins (leaching layers) and extra skins

Figure 36 shows the predicted volumetric change (top), and volumetric closure normalized to initial cavern volume (2nd panel), maximum σ_1 (3rd panel), and minimum *DF* (bottom) in the salt volume surrounding BH-113 over time. The initial cavern cavity volume was 12.9 MMB on 5/21/1991 and is predicted to be 12.0 MMB on 8/20/2022. The cavern volume is predicted to decrease by 6.9% over 31 years (5/21/1991 - 8/20/2022).

The maximum σ_1 never reaches a positive (tensile stress state) value through five drawdowns, and the minimum *DF* either never reaches to be less than 1 during every workover until the end of simulation. The largest predicted value of the maximum σ_1 is -438 psi on 3/21/2047 during the workover started on 1/1/2047 for three months. The smallest predicted value of the minimum *DF* is 2.26 on 11/20/1995 during the workover started on 10/25/1995 for 333 days.

In conclusion, BH-113 is predicted to be structurally stable through the fifth drawdown leach.

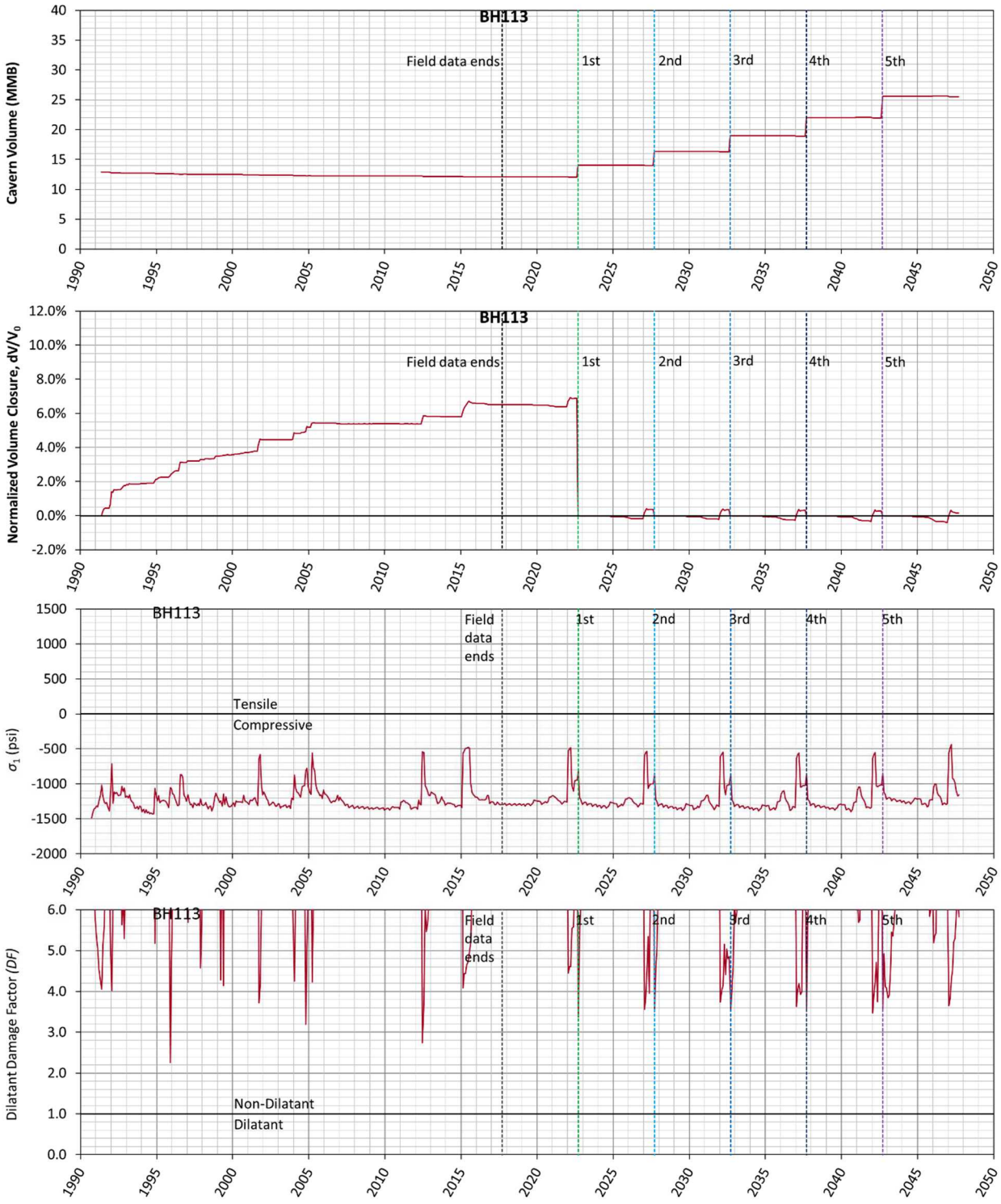

Figure 36. Predicted volumetric change (top), volumetric closure normalized to initial cavern volume of BH-113 (2nd), maximum σ_1 (3rd) and minimum dilatant damage factor (bottom) in the salt surrounding BH-113 over time

5.14. BH-114

Modeling of the leaching process of the caverns is performed by deleting a pre-meshed block of elements along the walls of the cavern so that the cavern volume is increased by 16 percent per drawdown. Figure 37 shows the cavity of BH-114 as developed from sonar data, along with drawdown skins and extra skins. In this simulation, BH-114 is modeled as having five drawdown layers to be removed to account for the future oil drawdown activities.

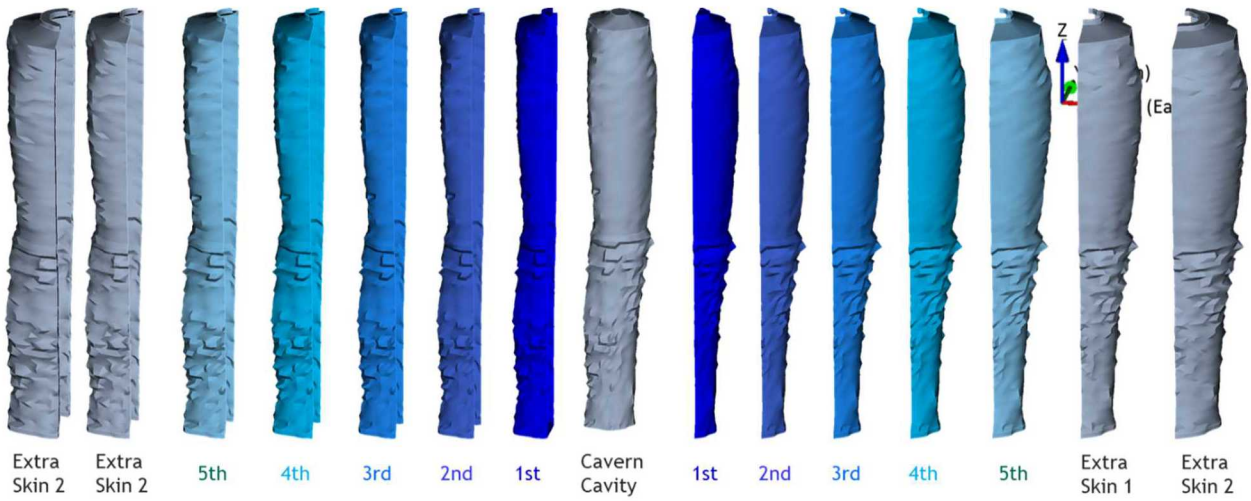

Figure 37. BH-114 cavern cavity with five drawdown skins (leaching layers) and extra skins

Figure 38 shows the predicted volumetric change (top), and volumetric closure normalized to initial cavern volume (2nd panel), maximum σ_1 (3rd panel), and minimum *DF* (bottom) in the salt volume surrounding BH-114 over time. The initial cavern cavity volume was 13.6 MMB on 8/20/1991 and is predicted to be 12.7 MMB on 8/20/2022. The cavern volume is predicted to decrease by 6.2% over 31 years (8/20/1991 - 8/20/2022).

The maximum σ_1 never reaches a positive (tensile stress state) value through five drawdowns, and the minimum *DF* either never reaches to be less than 1 during every workover until the end of simulation. The largest predicted value of the maximum σ_1 is -169 psi on 4/20/2013 during a series of workovers started on 9/8/2012 for 224 days. The smallest predicted value of the minimum *DF* is 1.60 on the same day of predicting the largest value of the maximum σ_1.

In conclusion, BH-114 is predicted to be structurally stable through the fifth drawdown leach.

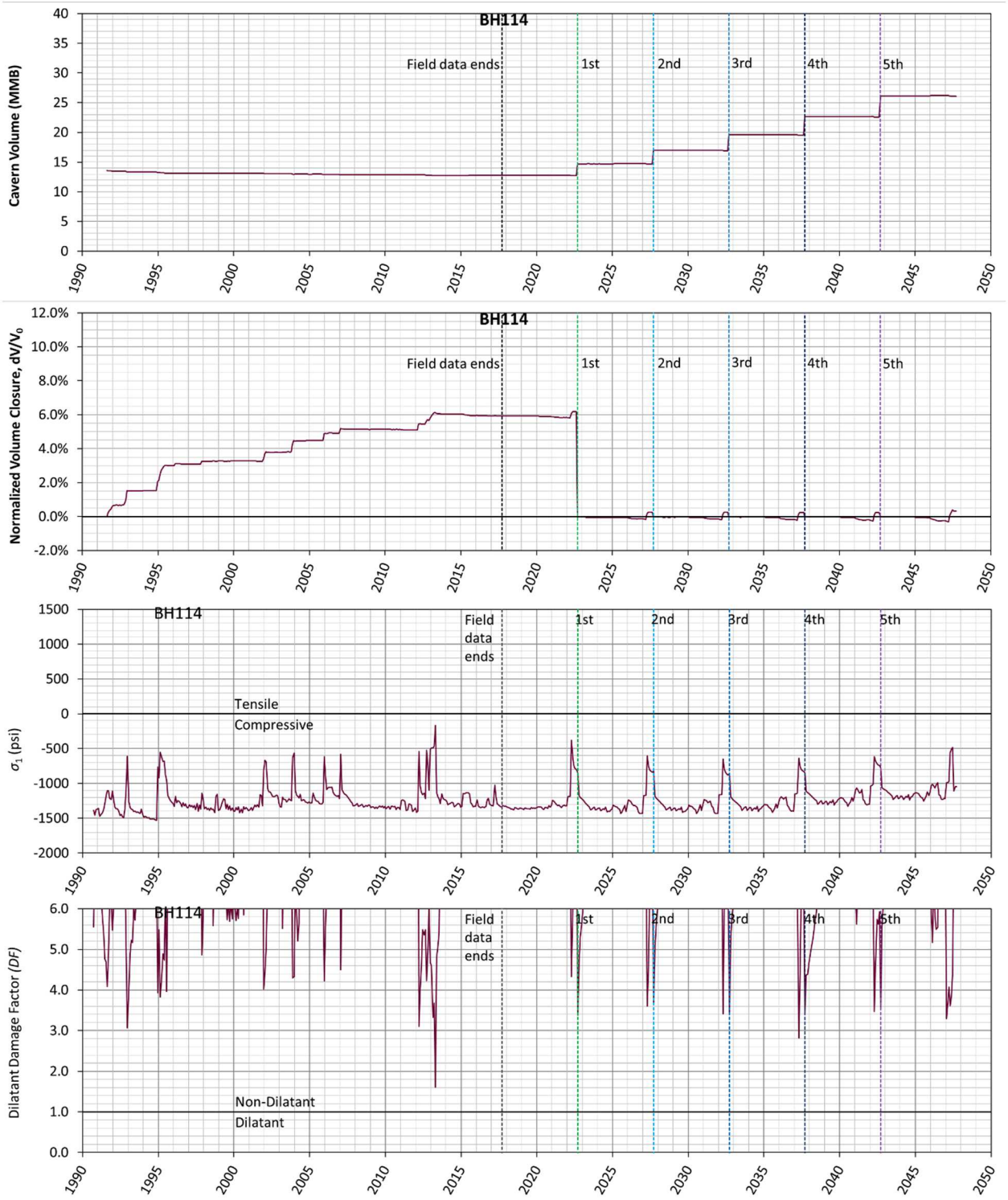

Figure 38. Predicted volumetric change (top), volumetric closure normalized to initial cavern volume of BH-114 (2nd), maximum σ_1 (3rd) and minimum dilatant damage factor (bottom) in the salt surrounding BH-114 over time

6. CONCLUSIONS - AVAILABLE DRAWDOWNS

The estimates for the baseline available drawdowns for each of the Big Hill caverns have been updated based on the recently upgraded Big Hill geomechanical model [Park, 2019b]. The new estimates for Big Hill are summarized in Table 2. All caverns are predicted to have five baseline available drawdowns remaining from a geomechanical perspective.

BH-101 and 105 have a region of concern at the floor edge and/or on the sloping floor, where tensile and dilatant stresses are predicted to occur during each workover. The tensile state is predicted to occur because of the geometries of the edge and floor. Therefore, geomechanical examination for two caverns would be recommended after a future drawdown leach.

The well integrity of each cavern is not investigated in this report. Only the structural integrity of the caverns is examined at this time. The number of available drawdowns in Table 2 is may be updated after the examination of the well integrity is completed through the upgraded BH geomechanical model next fiscal year. Such an update will incorporate a future Sandia strategy on how well integrity will affect drawdown capacity.

Table 2. 2020 Updated number of available drawdowns – Big Hill

Cavern	Basis in 2014				Updated Geomechanics in 2020	Remarks
	2D P/D < 1	3D P/D < 1	Geomechanics	Best Estimate		
BH-101	3	3	5	3	5	Re-examine after a drawdown
BH-102	4	4	5	4	5	
BH-103	2	4	5	4	5	
BH-104	3	3	5	3	5	
BH-105	4	4	5	4	5	Re-examine after a drawdown
BH-106	4	4	5	4	5	
BH-107	3	4	5	4	5	
BH-108	2	5	5	5	5	
BH-109	4	5	5	5	5	
BH-110	4	5	5	5	5	
BH-111	3	4	5	4	5	
BH-112	3	3	5	3	5	
BH-113	3	3	5	3	5	
BH-114	3	5	5	5	5	

REFERENCES

Ehgartner, B.L. and Bauer, S., 2004, Large Scale Salt Deformation: Comments on Subsidence using thermal, creep and Dissolution modeling to assess volumetric strain, SAND2004-0095C, Sandia National Laboratories, Albuquerque, NM 87185.

Lee, M.Y., Ehgartner, B.L., and Bronowski, D.R. (2004) *Laboratory Evaluation of Damage Criteria and Permeability of Big Hill Salt*, SAND2004-6004, Sandia National Laboratories, Albuquerque, NM 87185.

Hart, D.B. (2019), *Wellhead Pressure When Drawdown*, e-mail to B.Y. Park dated 10/30/2019, Sandia National Laboratories, Albuquerque, NM.

Park, B.Y., B.L. Ehgartner, M.Y. Lee, and S.R. Sobolik (2005) *Three Dimensional Simulation for Big Hill Strategic Petroleum Reserve (SPR)*, SAND2005-3216, Sandia National Laboratories, Albuquerque, NM.

Park, B.Y. and B.L. Ehgartner (2011) *Allowable Pillar to Diameter Ratio for Strategic Petroleum Reserve Caverns*. Unlimited Release SAND2011-2896, Sandia National Laboratories, Albuquerque, NM 87185. U.S. Strategic Petroleum Reserve.

Park, B.Y. (2017a) *Geomechanical Simulation of Big Hill Strategic Petroleum Reserve – Model Calibration*, SAND2018-13783, Sandia National Laboratories, Albuquerque, New Mexico.

Park, B.Y. (2017b) *Assessment of the Available Drawdowns for Oil Storage Caverns at the Bayou Choctaw SPR Site*, Unlimited Release SAND2017-12757, Sandia National Laboratories, Albuquerque, NM.

Park, B.Y. (2019a) *Assessment of the Available Drawdowns for Oil Storage Caverns at the Big Hill SPR Site – Cavern Integrity*, Unlimited Release SAND2019-7005, Sandia National Laboratories, Albuquerque, NM.

Park, B.Y. (2019b) *Geomechanical Simulation of Big Hill Strategic Petroleum Reserve - Calibration of Model Containing Shear Zone*, Unlimited Release SAND2019-11696, Sandia National Laboratories, Albuquerque, NM.

Rudeen, D.K. and D.L. Lord (2013) *SPR Cavern Pillar-to-Diameter 2013 Update*, Letter Report to Gilbert Shank, DOE PMO dated October 1, 2013. Geotechnology & Engineering, Sandia National Laboratories. U.S. Strategic Petroleum Reserve.

Snider Lord, Anna C. 2019. *Big Hill Model Containing the Shear Zone*, e-mail to B.Y. Park on August 20, 2019.

Sobolik S.R., B.Y. Park, D.L. Lord, B. Roberts, and D.K. Rudeeen (2014) *Current Recommendations Regarding ECP PM-00449, Baseline Remaining Drawdowns for all SPR Caverns*. FY14 Sandia Geotechnical Support for U.S. Strategic Petroleum Reserve, Letter Report to Lisa Nicholson dated May 9, 2014., Sandia National Laboratories, Albuquerque, NM.

Sobolik, S.R. (2016) *Assessment of the Available Drawdowns for Oil Storage Caverns at the West Hackberry SPR Site*. Unlimited Release SAND2016-3077, Sandia National Laboratories, Albuquerque, NM 87185.

Sobolik, S.R., D. Hart, B.Y. Park, and K. Chojnicki (2018) *Proposed Methodology for Assessing Available Drawdowns for Each Oil Storage Cavern in the Strategic Petroleum Reserve*, Unlimited Release SAND2018-4518, Sandia National Laboratories, Albuquerque, NM 87185.

DISTRIBUTION

Hardcopy—Internal

Number of Copies	Name	Org.	Mailstop
5	Carolyn L. Kirby	8862	MS0750
10	Byoung Y. Park	8862	MS0751

Email—External (encrypt for OUO)

Name	Company Email Address	Company Name
Wayne Elias	wayne.elias@hq.doe.gov	U.S. Department of Energy Office of Fossil Energy Washington, DC
Diane Willard	diane.willard@spr.doe.gov	U.S. Department of Energy SPR Project Management Office New Orleans, LA

Email—Internal

Name	Org.	Sandia Email Address
Erik K. Webb	8860	ekwebb@sandia.gov
Kirsten Chojnicki	8862	kchojni@sandia.gov
Donald M. Conley	8862	dconley@sandia.gov
Dylan Michael Moriarty	8862	dmmoria@sandia.gov
Anna C. Snider Lord	8862	acsnide@sandia.gov
Barry L. Roberts	8862	blrober@sandia.gov
Steven R. Sobolik	8862	srsobol@sandia.gov
David Hart	8862	dbhart@sandia.gov
David Lord	8865	dllord@sandia.gov
Giorgia Bettin	8866	gbettin@sandia.gov
Technical Library	1977	libref@sandia.gov

This page left blank

Sandia National Laboratories is a multimission laboratory managed and operated by National Technology & Engineering Solutions of Sandia LLC, a wholly owned subsidiary of Honeywell International Inc. for the U.S. Department of Energy's National Nuclear Security Administration under contract DE-NA0003525.